Dear Dr. Tina Treude and Dr. Marilaure Grégoire,

First, we respond specifically to the points raised by Dr. Treude, and then point-by-point to the reviews, and then list the major changes. Our responses are indicated in bold. A version of the manuscript with changes tracked is included at the end of this document. We apologize for the slight delay in the resubmission of our revised manuscript and thank you for your oversight of our manuscript. We believe that the thoughtful feedback from the reviewers has resulted in an improved manuscript and we hope that these changes make the manuscript acceptable for publication in *Biogeosciences*.

Sincerely,

Dr. Natalya Gallo, on behalf of co-authors

Comments from Dr. Treude:

"I support the suggestion to include Fig 2 (the detailed technical drawing) in the main manuscript."

We have included the technical drawing as Figure 2.

"I agree to keep Fig. 1D to show how the lander can be deployed from small boats."

Thank you, we have kept this image in.

"I support the suggestion from the external comment to include a supplementary table with fish species observed and min/max depths."

We have added this table as Supplement 1C.

"Please make sure to elaborate on the battery run time depending on the measurement settings as asked by reviewer #2. I believe this is an information many readers working in this field will appreciate."

We have elaborated on this in two sections. First, in the results:

"Memory and power capacity often limit deployment times for long-term, deep-sea deployments. In this study, the main technological limitation we ran into was limited battery capacity to power the LED lights. As opposed to 8 hours of estimated LED performance time, field performance ranged from 2.2 to 6.6 hours total time, which meant that the total time of biological data collection was shortened and ranged from 5.5 to 16.5 days, respectively (Table 1). Memory and power were not issues for the camera system; the 128 GB micro SD card was cleared and the battery pack was fully recharged following each deployment. Video quality was high enough to allow species-level identifications and the light from the LEDs was sufficient to light the field of view (Fig. 1F and G). The SeaBird MicroCAT-ODO also performed without any issues and had sufficient battery and memory capacity for all deployments. If not for power limitations to the LED lights, the camera system and SBE MicroCAT would have allowed for longer sampling (~1 month and potentially longer). The basic Nanolander itself can stay *in situ* for up to two years. Detailed descriptions of Nanolander performance can be found in Gallo (2018)."

Additionally, in the new concluding remarks section, we added the following:

"Our deployment lengths were limited by battery capacity to power the LED lights; all other elements would have allowed for longer sampling duration. Specific ways to extend future deployment lengths are currently being explored and include: using higher efficacy LEDs, integrating additional batteries to power the LED lights into newly devised Nanolander side pods, improving circuit performance that powers the LED lights by using new camera controllers and solid-state relays, and using low-light cameras, such as the Sony 7S II, which reduce the light required to illuminate the field of view. Longer deployment lengths would be advantageous for capturing ecosystem responses to environmental variability across time-scales (hours to months)."

Responses to Reviewers:

Reviewer 1 (SungHyun Nam)

1) What is the bottom topography around the Nanolanders? Table 1 well summarizes the seven deployments including information on deployment location and depth. But, 'Scripps Coastal Reserve', 'Del Mar Steeples Reef' with latitudes/longitudes and bottom depth are not enough information for readers (particularly someone who is not familiar to the region) to figure out local bathymetric features, where outer shelf and upper slope are located/ranged/shaped, seafloor area exposed to different oxygen conditions, and so on. It is important to give details of the bathymetry around the de- ployment sites highlighting the key information as mentioned above. This would also be helpful for better discussing physical drivers of the oxygen variability. Thus, I would like to suggest to add one figure (or incorporated into Figure 1) showing compact and easy to understand map of the local bathymetry along with the deployment locations."

We have created a new figure (Fig. 3) which clearly shows the deployment locations (green diamonds) in relationship to local bathymetric features. Despite relatively close spatial proximity between the Scripps Reserve and Del Mar deployment sites (~10 km), there are important bathymetric differences. The Scripps Coastal Reserve deployment sites are positioned close to a submarine canyon feature (the La Jolla canyon), while the Del Mar Steeples Reef deployment sites are on a gradually sloping margin. Additionally, we have added the locations of nearby CalCOFI stations (93.3 26.7 and 93.3 30) (black circles) and have included data from CalCOFI station 93.3 30 to provide additional context regarding variability over longer timescales.

The manuscript now reads:

"Seven deployments were conducted during the study period, ranging from 15-35 days, and at targeted depths of 100-400 m (Table 1). Two early deployments (D200-LJ-1 and D200-LJ-2) were done near the Scripps Reserve off La Jolla, CA and five subsequent deployments (D100-DM-Fall, D200-DM, D300-DM, D400-DM, D100-DM-Spr) targeted a nearby rockfish habitat – the Del Mar Steeples Reef, CA (Fig. 3). Despite relatively close spatial proximity (~10 km), the local bathymetry differed between the LJ and DM deployments (Fig. 3); the LJ deployments were close to a submarine canyon feature, while the DM deployments were on a gradually sloping margin."

2) There is no summary/concluding remarks/conclusion in the manuscript. Substantial conclusions are reached but they are not presented as a separate section. Thus, I would like to suggest to add Section 5 to conclude or summarize the materials.

We have modified what was previously section 4.3 of the discussion, titled “A global array of deep sea landers”, added additional content summarizing the findings of the study, and titled this section: "Section 5: Concluding remarks". This section now reads:

“Ocean deoxygenation is a global concern, with changes in oxygen conditions potentially impairing the productivity of continental shelves and margins that support important ecosystem services and fisheries. Nanolanders provide a powerful tool to examine short-term, fine-scale fluctuations in nearshore dissolved oxygen and other environmental parameters, and associated ecological responses that are rarely recorded otherwise. Oxygen variability was strongly linked to tidal processes, and contrary to expectation, high-frequency oxygen variability did not decline linearly with depth. Depths of 200 and 400 m showed especially high oxygen variability and seafloor communities at these depths may be more resilient to deoxygenation stress because animals are exposed to periods of reprieve during higher O2 conditions and may undergo physiological acclimation during periods of low O2 conditions at daily and weekly timescales. Despite experiencing high oxygen variability, seafloor communities showed limited responses to changing conditions at these short timescales. However, our deployments did not capture any large acute changes in environmental conditions that may elicit stronger community responses; future studies using this platform could allow for such observations.

The Nanolander DOV BEEBE is configured to collect paired physical, biogeochemical, and biological data in the deep-sea over multiple days, which is a rarity except for in areas with developed ocean observatories. We found that DOV BEEBE performed well over the course of the deployments, and allowed us to study seafloor community responses to short-term environmental forcing. Our deployment lengths were limited by battery capacity to power the LED lights; all other elements would have allowed for longer sampling duration. Specific ways to extend future deployment lengths are currently being explored and include: using higher efficacy LEDs, integrating additional batteries to power the LED lights into newly devised Nanolander side pods, improving circuit performance that powers the LED lights by using new camera controllers and solid-state relays, and using low-light cameras, such as the Sony 7S II, which reduce the light required to illuminate the field of view. Longer deployment lengths would be advantageous for capturing ecosystem responses to environmental variability across time-scales (hours to months).

Many of the areas where large decreases in oxygen have been observed occur in developing countries, such as along the western and eastern coast of Africa (Schmidtko et al. 2017). Large oxygen losses have also been observed in the Arctic (Schmidtko et al. 2017), where the seafloor habitat is understudied. Due to their compact design, small landers such as DOV BEEBE can provide a cost-effective and easily deployable tool for studying nearshore, deep-sea ecosystems and thus expand the capacity of developed and developing countries to monitor and study environmental changes along their coastlines. For continental margins and seafloor habitats, a global array of Nanolanders, similar in scope to the Argo program, could be envisioned. These would provide coupled physical, biogeochemical, and ecological measurements, which would greatly expand our understanding of temporal and spatial heterogeneity in nearshore deep-sea ecosystems and seafloor community sensitivity to environmental change.”

3) To give proper credit to related work, I would like to suggest to use '13CW', name of specific water mass linked to the deoxygenated water, instead of its locally defined water types, Pacific Equatorial Water (PEW) although previous works used the terms PEW. Based on recent work (Zachary et al., 2020; "The role of water masses in shaping the distribution of redox active compounds in the Eastern Tropical North Pacific oxygen deficient zone and influencing low oxygen concentrations in the eastern Pacific Ocean" published in Limnology and Oceanography as of 06 February 2020), two water masses – 13CW and deeper North Equatorial Pacific Intermediate Water (NEPIW) act as the two Pacific Equatorial source waters to the California Current System corresponding to upper and lower PEW at isopycnals of 26.2-26.8 kg m-3 when defined locally. Here, the relevant water mass seems to be 13CW (upper PEW), and not NEPIW (lower PEW).

Thank you for drawing our attention to this new reference. We have added the following clarification in the manuscript:

In Section 2.2: "Previous studies have found that changes in oxygen and pH in the Southern California Bight are associated with changes in the volume of Pacific Equatorial Water (PEW) transported in the California Undercurrent (Bograd et al. 2015, Nam et al. 2015). PEW is characterized by low oxygen, warm, high salinity conditions, and is composed of two water masses, the 13°C water mass (13CW) and the deeper Northern Equatorial Pacific Intermediate Water Mass (NEPIW) (Evans et al. 2020)."

To maintain consistency with the nomenclature in the reference, we have kept the use of "PEW" in cases where it directly refers to the results of a study. For example, "Previous studies have found that changes in oxygen and pH in the Southern California Bight are associated with changes in the volume of Pacific Equatorial Water (PEW) transported in the California Undercurrent (Bograd et al. 2015, Nam et al. 2015)."

But have otherwise used the 13CW terminology when referencing this water mass in the paper.

4) The observed oxygen variability over short time scales was compared with multi- decade-long deoxygenation or long-term trends/shifts reported in Bograd et al. (2008) and McClatchie et al. (2010). However, it was not discussed in comparison to inter-annual oxygen variability in the region. Does the period of data collection from August 2017 to March 2018 correspond to normal or more likely abnormal (El Niño/La Niña) year? My suggestion is to provide discussions on the observational results in terms of significant local interannual oxygen variability in association with such large-scale condition presented in Nam et al. (2011; "Amplification of hypoxia and acidic events by La Niña conditions on the continental shelf off California" published in Geophysical Research Letters as of 23 November 2011).

Thank you for this suggestion. Indeed, we were interested in comparing how short-term variability compares to longer-term variability driven both by interannual and multidecadal changes as one of the objectives of this research. To compare our high-frequency measurements to a longer-term dataset, we incorporated data from a nearby CalCOFI station to provide additional context to our results.

We have added the following to the manuscript:

"2.3 Short-term oxygen variability in the context of longer trends

To examine O_2 variability over shorter (i.e. daily and weekly) timescales compared to longer (i.e. seasonal, interannual, multidecadal) timescales, we compared our Nanolander results with the annual rates of oxygen loss reported for the SCB nearshore region (Bograd et al. 2008) as well as CTD casts from nearby CalCOFI station 93.3 28 (Fig. 3). CalCOFI station 93.3 26.7 was also nearby, but was too shallow for comparison with the Nanolander deployments (Fig. 3). Quality controlled CTD casts from station 93.3 28 were available for a ~16-year period (Oct 2003-November 2019), representing data from 61 cruises (calcofi.org). CTD data were used to examine characteristics of variability of temperature and oxygen through the water column, including mean conditions, the standard deviation, and the coefficient of variation across the 16-year period of quarterly samples. Oxygen data at 100, 200, 300, and 400 m were extracted to compare the distribution of observations across this 16-year period with the high-frequency measurements from the ~3-week Nanolander deployments. Additionally, we tested for significant linear trends in temperature or oxygen at 100, 200, 300, and 400 m, to examine recent (2003-2019) warming and deoxygenation trends at the CalCOFI station closest to the Nanolander deployments."

We have then provided these additional CalCOFI data as context for the Nanolander data within the revised discussion section: 4.1 Comparing oxygen variability: Short-term to long-term trends. The new additions read:

"CalCOFI data from nearby station 93.3 28 provides additional context on the characteristics of oxygen variability across seasonal and interannual timescales. When temperature and oxygen profiles from ~16 years of quarterly CalCOFI cruises are examined, we see that the highest temperature variability occurs in the upper water column (<50 m) and variability below ~150 m is relatively low (Fig. 7A,B). In contrast, absolute oxygen variability (i.e. standard deviation) is greatest between 50-150 m (Fig. 7C), and the coefficient of variation for oxygen (CV) actually increases below 100 m (Fig. 7D).

Comparing our high-frequency Nanolander deployment results to oxygen measurements across these ~16 years of quarterly CalCOFI cruises, we observe that the range in oxygen measurements at ~100 m, 300 m, and 400 m only captured a small portion of the variability measured across the ~16 year time period. In contrast, for the ~200 m deployments, a significant fraction of the variance over seasonal and interannual time-periods was captured by the short-term deployments (Fig. 7E-H). Oxygen variability in the SCB is also affected by the El Niño Southern Oscillation (ENSO), with oxygen conditions lower during La Niña periods (Nam et al. 2011). During the Nanolander deployments (August 2017-March 2018), the monthly Niño-3.4 index was always negative (-0.21 to -1.04; cpc.ncep.noaa.gov) but weaker than the La Niña conditions described in Nam et al. (2011). Our deployments, therefore captured a neutral ENSO/weak La Niña state. Interannual variability due to ENSO is captured in the data distribution from the CalCOFI cruises.

In recent years (2003-2019), at the CalCOFI station closest to the Nanolander deployments (93.3 28), no significant linear deoxygenation trends were detected at 100 or 200 m, but significant deoxygenation trends were detected for 300 and 400 m (300 m: LR, $R^2 = 0.10$, $p < 0.001$; 400 m: LR, $R^2 = 0.21$, $p < 0.001$) (Fig. 7J). No significant warming trends were detected at these depths during this period (Fig. 7I). At 300 m, oxygen declined by 0.89 µmol kg^{-1} $year^{-1}$ during the ~16 year time period, leading to a total oxygen loss of 14.25 µmol kg^{-1} across the timeseries, and at 400 m oxygen declined by 0.94 µmol kg^{-1} $year^{-1}$, leading to a total oxygen loss of 15.11 µmol kg^{-1} over the ~16 years. Comparatively, the range of oxygen conditions experienced

over the ~3-week Nanolander deployment was ~19 µmol kg^{-1} at 300 m and ~17 µmol kg^{-1} at 400 m."

A new figure was also produced and the figure caption reads:

"Figure 7: Comparing short-term environmental variability from *DOV BEEBE* deployments to longer-term trends using CTD casts at nearby CalCOFI station (93.3 28.0). Mean temperature (A) and oxygen (C) conditions through the water column (0-500 m) using CalCOFI CTD casts from Oct 2003-November 2019; light and dark colors indicate the variance around the mean and represent +/- 1 and 2 SD, respectively. Panels B and D show how the coefficient of variation (CV) for temperature and oxygen changes through the water column. Dotted lines in A-D indicate 100, 200, 300, and 400 m depths, and data are extracted for these depths for E-J. In E-H, violin plots show data distribution of oxygen measurements from ~16 years of CalCOFI quarterly cruises compared to ~3 week Nanolander deployments at 100 m (E), 200 m (F), 300 m (G), and 400 m (H). Violin plots show the mean +/- 1 SD (white) and +/- 2 SD (black). Panels I and J examine changes in temperature (I) and oxygen (J) conditions through time at 100, 200, 300, and 400 m. Dotted lines indicate non-significant linear relationships; solid lines indicate significant trends ($p < 0.05$)."

5) What are depths of thermocline/oxycline (any strong vertical temperature/oxygen gradient close to 200 m?) and their sectional structures across the shelf-slope? It would be helpful to check the cross-sectional structures of water temperature and dis- solved oxygen across the shelf and slope at a given time, e.g., see Figure 2 of Nam et al. (2011) but focusing on the deeper area (over the slope). Both mean and standard deviation to the mean, thus the CV of the temperature/oxygen can be partly explained from its vertical (and horizontal) gradient. My question is whether relatively high CV is due to strong vertical (or horizontal) gradient of temperature and oxygen (thermocline and oxycline depths). Also, how the structures are different from spring (D100-DM-Spr) vs. fall (DM100-DM-Fall)? It would also be relevant to high turbidity condition around 300 m as the internal waves/internal tides break and enhance the mixing (to resuspend the sediment) when and where the isopycnals (isotherms) touch the bottom (see the comments #6 below for details).

To look at patterns in cross-sectional structures of water temperature and dissolved oxygen across the shelf and slope, and to look at how these spatial patterns change seasonally, we extracted data from CalCOFI stations 93.3 28, 93.3 30, 93.3 35, and 93.3 40 and examined the CTD profiles for these stations during the deployment period. Four cruises were relevant to examine, however, cruise 1802SH was shortened due to the government shutdown and therefore only one of the four stations (93.3 30) was sampled. As such, we focused this additional analysis on just the three cruises (1708SR – August 2017, 1711SR – November 2017, and 1804SH – April 2018).

We created a new supplementary figure (Supplementary 1G) in which we show the temperature and oxygen profiles for these four stations across the three relevant cruises. From these profiles, we see that in the spring (April 2018), there is no onshore- offshore gradient, whereas in summer (August 2017) and to a lesser degree in late fall (November 2017), spatial differences in onshore (93.3 28 and 93.3 30) and offshore (93.3 35 and 93.3 40) environmental profiles are evident. These spatial differences are most pronounced in late summer (August 2017). Additionally, in August 2017 there is evidence of some unusual vertical structure in the oxygen profile around ~200 m; both at station 93.3 28 and 93.3 30. Our first deployment (D200-LJ-1) was conducted in late August, so may have captured part of this feature. However, this cannot fully explain the higher

variability we observed at 200 m, because our later deployment (D200-DM) was done in mid November, when there is no evidence of unusual vertical structure in the oxygen profile at 200 m for 93.3 28 or 93.3 30. These supplementary profiles, as well as the profiles in Figure 7 do show that the thermocline is steeper and shallower, overall, than the oxycline. We hope these additional datapoints help shed light on the sources of observed variability in our short-term deployments.

6) As described in Abstract, the high-frequency oxygen variability was strongly linked to tidal processes. But, I do not understand why it is contrary to expectation. As described in Section 1 (Lines 54-57), Section 3 (Lines 308-313), Section 4 (Lines 449-450 and 479-480), and Supplements, diurnal and semidiurnal oxygen variability is noticeable. This is not something unexpected but consistent with previous works reporting oxygen variability in a shallower zone, e.g., Frieder et al. (2012). Importance of tidal processes may also be confirmed from spring-neap cycles or modulations of semidiurnal/diurnal oxygen fluctuations. I could see such a spring (neap) amplification (reduction), for example, from time series plot of D10 - 98 m or D100-DM-Spr in Supplement 1B. Amplitudes of semidiurnal oxygen fluctuations reach up to larger than 20 μmol kg-1 for Days 0-3 and 10-13 (presumably corresponding to spring tide) while smaller than 10 μmol kg-1 for Days 5-8 and 17-20 (presumably corresponding to neap tide). What are CVs for periods of spring vs neap tides? I believed and continue to believe that such high-frequency oxygen variability is relevant to internal tides generated and shoaled at a specific phase of the surface tide in a sloping bottom (even up to the zone as shallow as 15 m) as reported in the region by Nam and Send (2011) and others. It is generally known that the isotherms (so iso-oxygen surfaces) move up and down at high-frequency due to propagation and evolution internal tides and associated shorter period nonlinear internal waves (also termed internal solitary waves). When they shoal and break, turbulent mixing is markedly enhanced often forming bottom nepheloid layer that may account for suspended sediments and the high turbidity condition around 300 m. The bottom nepheloid layer has been presented since McPhee-Shaw (2006; "Boundary-interior exchange: Reviewing the idea that internal-wave mixing enhances lateral dispersal near continental margins" published in Deep Sea Research II: Topical studies in Oceanography as of 20 February 2006), e.g., Boegman and Stastna (2019; "Sediment resuspension and transport by internal solitary waves" published in Annual Reviews of Fluid Mechanics as of 15 August 2018).

Thank you for raising these points. One of the objectives of this study was to place rates of anthropogenic change within the context of short-term variability that nearshore deep-sea communities are exposed to. These results show that tidally-driven variability is an important source of high-frequency variability to consider, that could either exacerbate or buffer deep-sea communities from changes in mean conditions with climate change. Contrary to the idea that the deep-sea is a stable environment, these results show a substantial amount of environmental variability occurring at short timescales on the upper margin.

As suggested by the reviewer, we examined the CVs for the two time periods specified by the reviewer for D100-DM-Spr. The CVs for the two time periods corresponding to the amplified oxygen pattern (Days 0-3 and Days 10-13) were 5.02% and 4.76%, respectively, while the CVs for the two time periods corresponding to the reduced oxygen variability (Days 5-8 and 17-20) were 2.66% and 2.69%, respectively.

However, contrary to expectation, a closer examination of the depth time series revealed that there was no consistent evidence that increased tidal amplitude gave rise to increased oxygen variability. We have added additional figures showing the oxygen and depth time series side by side for each deployment in Supplement 1F. For D100-DM-Spr, the initial period of high oxygen

variability (Days 0-3) corresponded to lower tidal amplitudes, and at the end of the deployment, the period of reduced oxygen variability (Days 17-20) corresponded to high tidal amplitudes.

Furthermore, we have examined this point by calculating the total daily range in oxygen concentration (i.e. daily maximum-daily minimum measurement) and daily range in depths for each deployment and examined if there is evidence of a positive correlation, which would suggest that increases in tidal amplitude (for example during a spring tide) would give rise to increased oxygen variability (as suggested by the reviewer). In fact, we have found the opposite to be true for certain deployments. For deployments D100-DM-Spr, D200-LJ-1, and D200-LJ-2 a negative relationship between tidal variability and oxygen variability can be seen. For D200-DM a weak negative relationship can be seen. For D100-DM-Fall, D300-DM, and D400-DM there is no relationship between tidal variability and oxygen variability. A figure with these results is included in Supplement 1F. These results are quite counterintuitive, and given that our expertise is not in physical oceanography, we do not feel comfortable speculating about the mechanism underlying these observed patterns. It is notable that the deployments that had negative relationships between tidal amplitudes and oxygen variability (Supplement 1F) are the same four deployments that show a clear negative relationship between spiciness and oxygen concentration (Fig. 5). As such, it may have something to do with the California Undercurrent and Pacific Equatorial Water. Perhaps during periods of higher tidal amplitude, the stratification between water masses is slightly reduced, leading to less overall oxygen variability during the tidal cycle. But, again, we do not feel comfortable speculating in the manuscript because this is not our area of expertise. The results are consistent when looking at the relationship between daily patterns of oxygen and tidal variability by calculating the CV, as opposed to looking at the range, so we are confident that the results are robust, though we are not sure how to explain them.

We have added the following section to the manuscript results: "Oxygen variability does not appear to increase with tidal amplitude; for D100-DM-Spr, D200-LJ-1, and D200-LJ-2 the daily oxygen range appears to be negatively correlated with the daily tidal range (Supplement 1F)."

We have also added the suggested references in the discussion in section 4.2:

"The high turbidity observed at 300 m may be due to shoaling and breaking nonlinear internal waves that can form bottom nepheloid layers (McPhee-Shaw 2006, Boegman and Stastna 2019). On the Peruvian margin, energy dissipation from tidally-driven internal waves have been shown to influence the distribution of epibenthic organisms by increasing suspension, transport, and deposition of food particles (Mosch et al. 2012). High turbidity conditions have also been observed during two separate ROV dives at ~340 m off Point Loma (unpublished, NDGallo), suggesting high turbidity conditions may be the norm at these depths on the upper slope in the SCB."

7) Not being a biologist, I do not know in detail how the seafloor communities respond to short-period (mostly diurnal) changes in environmental conditions, but it is convincing that longer time series data are vital for addressing the science issue. My question is why camera sample should be less frequent for longer-term deployment. Is it limited by battery or memory? There would be several technical ways to overcome battery or memory limit. Why not trying new technologies that allow longer-term deployment keeping the same camera (as well as other sensors) sampling frequency.

We have clarified this in the new conclusion section. The new text reads: "Our deployment lengths were limited by battery capacity to power the LED lights; all other elements would have

allowed for longer sampling duration. Specific ways to extend future deployment lengths are currently being explored and include: using higher efficacy LEDs, integrating additional batteries to power the LED lights into newly devised Nanolander side pods, improving circuit performance that powers the LED lights by using new camera controllers and solid-state relays, and using low-light cameras, such as the Sony 7S II, which reduce the light required to illuminate the field of view. Longer deployment lengths would be advantageous for capturing ecosystem responses to environmental variability across time-scales (hours to months)."

Reviewer 2 (Anonymous)

I very much like the idea of the small-sized and hand-operated lander and I fully agree with the need for such systems for the performance of more in situ long-term observations. Yet, given the actual size and weight of the lander, the expression 'Nanolander' seems a bit exaggerated. This is just a personal opinion and is by no means meant to urge the authors to change the name of their system. In this context, the last section of the MS "A global array of deep-sea landers" goes in the same direction and appears a bit superficial with an emphasis on "selling" the system. The authors might consider to rewrite this last section increasing its profoundness.

We agree in principle that the small benthic lander is not actually "nano", however, Nanolander is now a registered proper name that specifies this scientific platform, so we maintain the name in the manuscript. The term arose to distinguish it from much larger traditional benthic landers.

We appreciate the reviewer's perspective that the final section could be further expanded to increase its profoundness. Similarly, the first reviewer suggested we add a section of concluding remarks. As such, we have revised Section 4.3 of the discussion which was titled "A global array of deep sea landers", which is now titled Section 5: Concluding remarks. This section now reads:

"Ocean deoxygenation is a global concern, with changes in oxygen conditions potentially impairing the productivity of continental shelves and margins that support important ecosystem services and fisheries. Nanolanders provide a powerful tool to examine short-term, fine-scale fluctuations in nearshore dissolved oxygen and other environmental parameters, and associated ecological responses that are rarely recorded otherwise. Oxygen variability was strongly linked to tidal processes, and contrary to expectation, high-frequency oxygen variability did not decline linearly with depth. Depths of 200 and 400 m showed especially high oxygen variability and seafloor communities at these depths may be more resilient to deoxygenation stress because animals are exposed to periods of reprieve during higher O2 conditions and may undergo physiological acclimation during periods of low O2 conditions at daily and weekly timescales. Despite experiencing high oxygen variability, seafloor communities showed limited responses to changing conditions at these short timescales. However, our deployments did not capture any large acute changes in environmental conditions that may elicit stronger community responses; future studies using this platform could allow for such observations.

The Nanolander DOV BEEBE is configured to collect paired physical, biogeochemical, and biological data in the deep-sea over multiple days, which is a rarity except for in areas with developed ocean observatories. We found that DOV BEEBE performed well over the course of the deployments, and allowed us to study seafloor community responses to short-term environmental forcing. Our deployment lengths were limited by battery capacity to power the

LED lights; all other elements would have allowed for longer sampling duration. Specific ways to extend future deployment lengths are currently being explored and include: using higher efficacy LEDs, integrating additional batteries to power the LED lights into newly devised Nanolander side pods, improving circuit performance that powers the LED lights by using new camera controllers and solid-state relays, and using low-light cameras, such as the Sony 7S II, which reduce the light required to illuminate the field of view. Longer deployment lengths would be advantageous for capturing ecosystem responses to environmental variability across time-scales (hours to months).

Many of the areas where large decreases in oxygen have been observed occur in developing countries, such as along the western and eastern coast of Africa (Schmidtko et al. 2017). Large oxygen losses have also been observed in the Arctic (Schmidtko et al. 2017), where the seafloor habitat is understudied. Due to their compact design, small landers such as DOV BEEBE can provide a cost-effective and easily deployable tool for studying nearshore, deep-sea ecosystems and thus expand the capacity of developed and developing countries to monitor and study environmental changes along their coastlines. For continental margins and seafloor habitats, a global array of Nanolanders, similar in scope to the Argo program, could be envisioned. These would provide coupled physical, biogeochemical, and ecological measurements, which would greatly expand our understanding of temporal and spatial heterogeneity in nearshore deep-sea ecosystems and seafloor community sensitivity to environmental change."

As the paper claims to introduce a novel lander-technology, I would have wished to find a brief review of similar already existing systems. The authors mention papers by Jamieson et al. but do not provide details. Please add a few lines highlighting where your system goes beyond existing systems.

Thank you for highlighting this omission. We have added the following to the introduction:

"Untethered instrumented seafloor platforms, sometimes called "ocean landers", have a long and rich history (Ewing and Vine 1938, Tengberg et al. 1995). These vehicles are self-buoyant, with an expendable descent anchor that is released by surface command or on-board timer, allowing the vehicle to float back to the surface. Autonomous landers have several advantages for deep-sea research, such as lower cost combined with spatial flexibility. Unlike moorings or cabled observatories, small landers (< 2 m high) can easily be recovered using small boats and redeployed to new depths and locations (Priede and Bagley 2000, Jamieson 2016)."

We have also tried to highlight the specific novelty of the Nanolander design within Section 2.1 Nanolander development and deployment. This reads:

"Autonomous landers have been used successfully to observe abyssal and deep-sea trench communities (e.g., Jamieson et al. 2011, Gallo et al. 2015), however, these landers were large and required a ship with an A-frame and winch to deploy and recover. For this study, the goal was to develop a deep-water lander that could easily be hand-deployed out of a small boat and that was capable of continuously collecting hydrographic and fish and invertebrate assemblage data from near the seafloor for several weeks at a time…. The Nanolander frame is made of marine-grade high-density polyethylene (HDPE) (brand name "Starboard") and reinforced with fiberglass pultruded channel and angle beams for structure, reducing in-water weight. HDPE has a specific gravity of <1, close to neutrally buoyant. The specific gravity of fiberglass is 2/3 that of aluminium, requiring less flotation to achieve neutral buoyancy. Both plastic materials are impervious to saltwater corrosion…. The novel design aspects of the Nanolander include the use of plastic spheres for both instrument housing and flotation, which allow the vehicle to be smaller

and lighter. Previous generation landers, such as the landers used for the *DEEPSEA CHALLENGE* Expedition (Gallo et al. 2015), used syntactic foam for flotation, which is more expensive and requires a metal support frame. While glass spheres have a deeper maximum operational depth (to 11 km), the use of glass-filled polyamide spheres in the Nanolander has machining advantages and decreases the price point. The plastic spheres used for *DOV BEEBE* are pressure-tolerant to 1 km; new spheres with 20% glass content are pressure tolerant to 2 km… This battery system is novel and was developed specifically to fit within the spatial constraints of the sphere and provide high power capacity."

Beside oxygen, other parameters were measured (temperature, pH, saturation state of aragonite/calcite) but these were hardly mentioned in the discussion section although e.g. pH in respiration physiology is very important. Please clarify why these parameters were not further included in the interpretation of the data set.

We agree that temperature, pH, and saturation state of aragonite/calcite are important parameters to consider as well, and for this reason have included this data in the description of environmental variability across deployments. However, since oxygen and carbonate chemistry parameters co-vary (Alin et al. 2012), we are not able to decouple these in our interpretation of community-level differences in the dataset. Mobile, adult fishes are not as susceptible to low pH as to changes in oxygen availability (Melzner et al. 2009, Kroeker 2013), and we therefore make the assumption that respiratory demands play an important role in driving community responses.

Additional deployments, including longer-term deployments and repeat deployments at the same sites, would provide the opportunity to perform more in-depth analyses into the roles of different environmental drivers in giving rise to specific community responses. Additionally, we do not think that decreasing pH with depth is responsible for the observed shift from vertebrates to invertebrates, since many of the invertebrates at these deeper depths are calcifers, which should be more sensitive to low pH conditions.

Further comments and edits: Line 24: please explain "phest"

Changed to "estimated pH" instead of "pHest". This is a calculated pH using empirical relationships derived for this region in Alin et al. (2012). Within the manuscript, pHest is defined as: "pHest is estimated pH, calculated using empirical relationships from Alin et al. (2012)."

Line 67-72 in this context eddy correlation techniques could be mentioned

We have added: "Eddy correlation techniques are also used to measure non-invasive oxygen fluxes at the seafloor, however require ROVs or scuba divers to deploy (Berg et al. 2009)."

Line 108: suggest to use only metric units of m or cm instead of ft

Only metric units are now included. This section now reads, "DOV BEEBE stands 1.6 m tall and is 0.36 m wide and 0.36 m deep. . . Within the frame sit three plastic spheres that are 25.4 cm in diameter. . .. When DOV BEEBE is deployed, the vertical distance from the base of the Nanolander to the seafloor is ~51 cm (Fig. 1B)."

Figure 1, suggest to include a more detailed technical drawing of the lander (i.e. better version of Fig. 1A) where the different major components are labeled with numbers which can referred to in the main text. Figure 1D is not really providing any additional information and could be omitted. Please provide in the final version of the MS the figures in sufficient resolution.

We have provided an additional technical drawing of the lander as Figure 2. The caption that goes with the labels is as follows:

"Figure 2: A detailed schematic of the Nanolander *DOV BEEBE* components: 1) Spectra lifting bale; 2) High-density polyethylene (HDPE) centerplate; 3) ~25 cm polyamide spheres stacked top, middle and bottom, see description, Section 2.1; 4) sphere retainer; 5) auxiliary ~18 cm flotation sphere; 6) oil-filled LED lights; 7) Seabird MicroCAT-ODO in the lower payload bay; 8) central fiberglass frame; 9) stabilizing counterweight; 10) anchor slip ring; 11) expendable iron anchor (bar bell weights); 12) burnwire release and mount, one port side, one starboard side; 13) Edgetech hydrophone for acoustic command and tracking; 14) HDPE side panels; and 15) surface recovery flag. Not shown: drop arm on front (see Fig. 1B and 1E)."

We have kept Figure 1D within the manuscript figure because it showcases that the Nanolander fits exactly in a horizontal configuration within a Panga, or small boat. These types of boats are readily available all around the world and are typically used by artisanal and recreational fishermen. Thus being able to transport, deploy, and recover the Nanolander in these boats increases the potential for using this scientific platform in many regions of the world, both developed and developing.

Line 111: "glass filled" sounds a bit odd; do you mean glass-spheres housed by polyamide protective shells?

The plastic spheres are an injection-molded polyamide (nylon) with 15% glass fibers for additional strength. The composite approach is similar to FRP (Fiber Reinforced Plastic), or "Fiberglass", but using nylon as the binder, not polyester epoxy. We have clarified this in the manuscript and modified it to read, "Within the frame sit three plastic spheres that are 25.4 cm in diameter; the spheres are made of injection-molded polyamide with 15% glass fibers for additional strength."

Line 122: "The power supply for the BART board is housed in the upper sphere", together with the Bart board?

This is correct. A battery pack supplies the power to the BART board, and is housed in the upper sphere together with the BART board. We have clarified this to read, "The battery for the BART board is housed in the upper sphere with the BART board."

Line 123: what would be the maximum deployment time of DOV Beebe with the given battery systems?

We have added the following information to the manuscript. In the results section 3.1 Nanolander performance:

"Memory and power capacity often limit deployment times for long-term, deep-sea deployments. In this study, the main technological limitation we ran into was limited battery capacity to power

the LED lights. As opposed to 8 hours of estimated LED performance time, field performance ranged from 2.2 to 6.6 hours total time, which meant that the total time of biological data collection was shortened and ranged from 5.5 to 16.5 days, respectively (Table 1). Memory and power were not issues for the camera system; the 128 GB micro SD card was cleared and the battery pack was fully recharged following each deployment. Video quality was high enough to allow species-level identifications and the light from the LEDs was sufficient to light the field of view (Fig. 1F and G). The SeaBird MicroCAT-ODO also performed without any issues and had sufficient battery and memory capacity for all deployments. If not for power limitations to the LED lights, the camera system and SBE MicroCAT would have allowed for longer sampling (~1 month and potentially longer). The basic Nanolander itself can stay *in situ* for up to two years. Detailed descriptions of Nanolander performance can be found in Gallo (2018)."

And also in the 5.0 Concluding remarks section:

"Our deployment lengths were limited by battery capacity to power the LED lights; all other elements would have allowed for longer sampling duration. Specific ways to extend future deployment lengths are currently being explored and include: using higher efficacy LEDs, integrating additional batteries to power the LED lights into newly devised Nanolander side pods, improving circuit performance that powers the LED lights by using new camera controllers and solid-state relays, and using low-light cameras, such as the Sony 7S II, which reduce the light required to illuminate the field of view. Longer deployment lengths would be advantageous for capturing ecosystem responses to environmental variability across time-scales (hours to months)."

Line 131: would be nice if especially details of the camera system could better show up in the improved version of Figure 1A

We have provided the 10 page SphereCam manual as Supplement 1A.

Line 153: please use metric units

Changed to: "DOV BEEBE is positively buoyant in water, and is deployed with ~18 kg of sacrificial iron weights."

Line 178: I think there is no need to use the word "high-frequency" (it's rather a matter of the perspective whether 5 min sampling rate is high-frequency or not)

The word "high-frequency was removed". The sentence now reads:
"Upon recovery of the Nanolander, time-series data from the MicroCAT were analyzed to assess how environmental variability (O2, T, salinity) changes with depth."

Line 194 please describe spiciness in a bit more detail, it's likely not common to everybody

We have further clarified this in the text, which now reads: "Spiciness, the degree to which water is warm and salty, is a state variable that is conserved along isopycnal surfaces (Flament 2002) and can be used as a tracer for PEW (Nam et al. 2015). We calculated spiciness using the "oce" R package (Kelley and Richards 2017) and examined how oxygen concentration varies with temperature and spiciness across depths and deployments. Spiciness is used to examine

differences in spatial variation between water masses, which otherwise may not be apparent using isopycnal surfaces because the effects of warm temperature and high salinity cancel each other out. "Spicier" water is warmer and saltier."

Line 309 deconstructed time series - please explain in more detail

This was further clarified in the text, which now reads: "When the time series were decomposed into their additive components (i.e. daily trend, underlying trend, and random noise), time series for all depths showed a clear diurnal and semi- diurnal signal (Supplement 1E)."

We have also added a citation for the R package used for the decomposition in the Methods section:
"The oxygen time series for each deployment was also decomposed using the "stats" package (R Core Team 2019) to look at the trend, daily, and random signals that contribute to the overall data patterns."

Figure 4: the labels for "day" and "night" are difficult to read – please enlarge

We have enlarged the label sizes for day and night. This Figure is now Figure 6.

Line 448: I am not sure whether the statement "At ~200 m, oxygen, temperature, and pH exhibited high variability (Fig. 2), greater at times than the variability observed at 100 m." is correct for temperature – please check.

Thank you for pointing this out. I have taken a close look at Table 1 and inspected the overall ranges and CVs for the different deployments. For D200- DM, variability for temperature was higher than during D100-DM-Spr, based on the overall range and CV, but lower than during D100-DM-Fall. Temperature variability for D200-LJ-2 was very similar to temperature variability for D100-DM-Spr but also lower than D100-DM-Fall, based on overall range and CV (Table 1). D200-LJ-1 has lower temperature variability than both D100-DM-Spr and D100-DM-Fall.

I have clarified this in the results section, which reads: "While we expected that O2 variability would decrease with depth, instead we found that the greatest variability in oxygen conditions over these short time-scales was observed at ~200 m (Table 1). All three deployments from ~200 m showed broad probability density distributions of environmental conditions (Fig. 4) and large ranges in oxygen and pHest for the deployment period (Table 1). The average daily range in oxygen concentration (i.e. daily maximum-daily minimum) was highest for D200-LJ-2 (~34 µmol kg-1), followed by D200-LJ-1 (~31 µmol kg-1), followed by D200-DM (~24 µmol kg-1). The average daily oxygen range for both ~100 m deployments was lower (~20 µmol kg-1 for D100-DM-Fall and ~14 µmol kg-1 for D100-DM-Spr). The coefficient of variation (CV) for oxygen at ~200 m was twice higher than for the ~100 m deployments (Table 1). While deployments at ~300 m (D300-DM) and ~400 m (D400-DM) had much narrower probability density distributions of environmental conditions (Fig. 4), the ranges in oxygen and pHest at ~400 m were only slightly smaller than at ~300 m (Table 1). The CV for oxygen was higher at ~400 m (10.20%) compared to ~300 m (7.02%) (Table 1). The average daily range in oxygen concentration was ~11 µmol kg-1 for D300-DM and ~8 µmol kg-1 for D400-DM. Temperature did not exhibit the same pattern of variability as oxygen, with the highest variability (CV) observed during D100-DM-Fall (~100 m) (Table 1). Variability in pHest (CV) was almost twice higher at shallower depths (< 200 m), than

at ~300 or ~400 m (Table 1).

Although the Figure 2 is quite attractive and informative, especially for the discussion section, when environmental variability is discussed additional Box plots might be helpful to elucidate the differences between the different deployments (i.e. depths).

Thank you for your positive feedback on Figure 2. We have added additional violin plots for the oxygen measurements for each Nanolander deployment to a new figure (Figure 7), which additionally addresses question 4 raised by Reviewer 1. The violin plots also show the mean and +/- 1 and 2 standard deviation.

The Figure caption reads: "Figure 7: Comparing short-term environmental variability from *DOV BEEBE* deployments to longer-term trends using CTD casts at nearby CalCOFI station (93.3 28.0). Mean temperature (A) and oxygen (C) conditions through the water column (0-500 m) using CalCOFI CTD casts from Oct 2003-November 2019; light and dark colors indicate the variance around the mean and represent +/- 1 and 2 SD, respectively. Panels B and D show how the coefficient of variation (CV) for temperature and oxygen changes through the water column. Dotted lines in A-D indicate 100, 200, 300, and 400 m depths, and data are extracted for these depths for E-J. In E-H, violin plots show data distribution of oxygen measurements from ~16 years of CalCOFI quarterly cruises compared to ~3 week Nanolander deployments at 100 m (E), 200 m (F), 300 m (G), and 400 m (H). Violin plots show the mean +/- 1 SD (white) and +/- 2 SD (black). Panels I and J examine changes in temperature (I) and oxygen (J) conditions through time at 100, 200, 300, and 400 m. Dotted lines indicate non-significant linear relationships; solid lines indicate significant trends ($p < 0.05$)."

Line 476 Turbidity can be related to local hydrodynamics caused by the energy dissipa- tion of incipient internal tides at sloping boundaries affecting the suspension, transport and deposition of food particles. If you are interested, please see e.g. Mosch et al. (2012) Factors influencing the distribution of epibenthic megafauna across the Peruvian oxygen minimum zone. Deep-Sea Research I 68 (2012) 123–135 and references therein.

Thank you for pointing us to this interesting study. Similarly, Reviewer 1 also raised the importance of internal tides breaking on the margin as a source of environmental variability that may also explain the high turbidity conditions observed during our 300 m deployment.

In section 4.2 of our discussion, we have added suggested references from both reviewers. This new paragraph now reads, "The high turbidity observed at 300 m may be due to shoaling and breaking nonlinear internal waves that can form bottom nepheloid layers (McPhee-Shaw 2006, Boegman and Stastna 2019). On the Peruvian margin, energy dissipation from tidally-driven internal waves have been shown to influence the distribution of epibenthic organisms by increasing suspension, transport, and deposition of food particles (Mosch et al. 2012). High turbidity conditions have also been observed during two separate ROV dives at ~340 m off Point Loma (unpublished, NDGallo), suggesting high turbidity conditions may be the norm at these depths on the upper slope in the SCB."

List of all relevant changes made in the manuscript:

3 new figures:

- Fig. 2: A detailed schematic of the Nanolander DOV BEEBE
- Fig. 3: A map showing Nanolander deployment locations with relevant bathymetry (Fig. 3)
- Fig. 7: Figure comparing our short-term variability results from the Nanolander deployments with longer-term trends from CTD cast from a nearby CalCOFI station

Additional Supplementary Materials

- Supplement 1A: SphereCam manual
- Supplement 1C: Table of fish species observations
- Supplement 1F: Additional figures added to examine relationship between tidal amplitude and oxygen variability in response to reviewer 1
- Supplement 1G: Response to reviewer 1 about vertical and cross-shelf and slope structure in the water column during our deployment period.

Manuscript changes:

- General edits to improve readability
- Additional specificity on aspects of the nanolander that are novel to address Reviewer 2's request
- Modification of Fig. 6 to increase label sizes and update of Panel C.
- Addition of Section 2.3 Short-term oxygen variability in the context of longer trends (to address Reviewer 1's points about interannual variability)
- Significant rewrite of Section 4.1 Comparing oxygen variability: Short-term to long-term trends to incorporate comparison to CalCOFI station data (to address Reviewer 1's points about interannual variability)
- New Conclusion section (Section 5.0 Concluding remarks) added as requested by Reviewer 1, with specific additions as suggested by Reviewer 2
- Additional references added as suggested by reviewers, and to further develop points the reviewers asked to be addressed
- All code and data were uploaded to a Zenodo repository and the url is included in the manuscript "Code and Data availability" section. Data and code publication will be timed with manuscript acceptance and publication.

Characterizing deep-water oxygen variability and seafloor community responses using a novel autonomous lander

Natalya D. Gallo[1,2,3], Kevin Hardy[4], Nicholas C. Wegner[2], Ashley Nicoll[1], Haleigh Yang[5], Lisa A. Levin[3,5]

[1]Marine Biology Research Division, Scripps Institution of Oceanography, University of California San Diego, La Jolla, California 92093, USA
[2]Fisheries Resources Division, Southwest Fisheries Science Center, NOAA Fisheries, 8901 La Jolla Shores Drive, La Jolla, CA 92037, USA
[3]Center for Marine Biodiversity and Conservation, Scripps Institution of Oceanography, University of California San Diego, La Jolla, California 92093, USA
[4]Global Ocean Design LLC, 7955 Silverton Avenue Suite 1208, San Diego, CA 92126, USA
[5]Integrative Oceanography Division, Scripps Institution of Oceanography, University of California San Diego, La Jolla, California 92093, USA

Correspondence to: Natalya D. Gallo (ndgallo@ucsd.edu)

Abstract. Studies on the impacts of climate change typically focus on changes to mean conditions. However, animals live in temporally variable environments that give rise to different exposure histories that can potentially affect their sensitivities to climate change. Ocean deoxygenation has been observed in nearshore, upper-slope depths in the Southern California Bight, but how these changes compare to the magnitude of natural O_2 variability experienced by seafloor communities at short timescales is largely unknown. We developed a low-cost and spatially flexible approach for studying nearshore, deep-sea ecosystems and monitoring deep-water oxygen variability and benthic community responses. Using a novel, autonomous hand-deployable Nanolander with an SBE MicroCAT and camera system, high-frequency environmental (O_2, T, estimated pH) and seafloor community data were collected at depths between 100-400 m off San Diego, CA to characterize: timescales of natural environmental variability, changes in O_2 variability with depth, and community responses to O_2 variability. Oxygen variability was strongly linked to tidal processes, and contrary to expectation, oxygen variability did not decline linearly with depth. Depths of 200 and 400 m showed especially high O_2 variability; these conditions may give rise to greater community resilience to deoxygenation stress by exposing animals to periods of reprieve during higher O_2 conditions and invoking physiological acclimation during low O_2 conditions at daily and weekly timescales. Despite experiencing high O_2 variability, seafloor communities showed limited responses to changing conditions at these shorter timescales. Over 5-month timescales, some differences in seafloor communities may have been related to seasonal changes in the O_2 regime. Overall, we found lower oxygen conditions to be associated with a transition from fish-dominated to invertebrate-dominated communities, suggesting this taxonomic shift may be a useful ecological indicator of hypoxia. Due to their small size and ease of use with small boats,

Deleted: which
Deleted: could
Deleted: compared
Deleted: time-scales was
Deleted: aimed to develop
Deleted: pHest
Deleted: which may buffer communities at
Deleted: depths
Deleted: them
Deleted: relatively high
Deleted: across short time-scales (
Deleted:).
Deleted: time-scales

hand-deployable Nanolanders can serve as a powerful capacity-building tool in data-poor regions for characterizing environmental variability and examining seafloor community sensitivity to climate-driven changes.

1 Introduction

Natural environmental variability can affect the resilience or sensitivity of communities to climate change. Communities and species living in variable environments are often more tolerant of extreme conditions than communities from environmentally stable areas (Bay and Palumbi 2014). For example, in seasonally hypoxic fjords, temporal oxygen variability influences seafloor community beta diversity patterns, and can allow certain species to live for periods of time under average oxygen conditions that are below their critical oxygen thresholds (P_{crit}) (Chu et al. 2018). In addition, the anthropogenic signal of deoxygenation takes a longer time to emerge in systems with higher natural oxygen variability (Long et al. 2016, Henson et al. 2017), such as Eastern Boundary Upwelling systems. Natural variability of dissolved oxygen at different timescales is therefore an important environmental factor to consider when studying the impacts of deoxygenation on communities.

While data on shallow-water O_2 and pH variability have proven valuable for interpreting faunal exposures (Hofmann et al. 2011b, Frieder et al. 2012, Levin et al. 2015), high-frequency measurements are rare below inner shelf depths. Specifically, datasets on organismal and community responses to environmental variability are rare for the deep sea; however, those that exist, are informative and illustrate a dynamic environment (Chu et al. 2018, Matabos et al. 2012). Studies from NEPTUNE (the North-East Pacific Time-Series Undersea Networked Experiments) in B.C. Canada show that even at 800-1000 m, fish behavior is linked to variations in environmental conditions across different temporal scales including day-night and internal tide temporalizations (Doya et al. 2014) and seasonal cycles (Juniper et al. 2013). Combined high-frequency quantitative sampling of environmental and biological data allows examination of which processes shape benthic communities (Matabos et al. 2011, 2014).

Currently, tools for studying deep-water, seafloor ecosystems include deep-submergence vehicles (HOVs, AUVs, and ROVs), towed camera sleds, and trawls. These approaches typically require significant resource investment, and the use of large ships with winch capabilities. Moorings and cabled observatories are also very useful; however, these are usually fixed to specific sites and are typically costly. Eddy correlation techniques are also used to measure non-invasive oxygen fluxes at the seafloor, however require ROVs or scuba divers to deploy (Berg et al. 2009).

Untethered instrumented seafloor platforms, sometimes called “ocean landers”, have a long and rich history (Ewing and Vine 1938, Tengberg et al. 1995). These vehicles are self-buoyant, with an expendable descent anchor that is released by surface command or on-board timer, allowing the vehicle to float back to the surface. Autonomous landers have several advantages for deep-sea research, such as lower cost combined with spatial flexibility. Unlike moorings or cabled observatories, small landers (< 2 m high) can easily be recovered using small boats and redeployed to new depths and locations (Priede and Bagley 2000, Jamieson 2016).

Deleted: constant

Deleted: In

Deleted: Pacific

Deleted: survive even when

Deleted: The

Deleted: also

Deleted: time scales

Deleted: No published high-frequency deep-water O_2 or pH measurements are available for depths below 100 m in the Southern California Bight (SCB). The California Cooperative Oceanic Fisheries Investigations (CalCOFI) long-term time series provides quarterly measurements showing decreases in oxygen conditions from 1984 to 2006 of up to 2.1 μmol kg^{-1} y^{-1} in the SCB, with a mean decrease of 21% below the thermocline at 300 m (Bograd et al. 2008, 2015). However, similar low oxygen levels were measured in the late 1950s and 60s (McClatchie et al.

Moved down [1]: 2010).

Deleted:

Moved down [2]: Notably, daily, weekly and even seasonal low oxygen extreme events (e.g. Send and Nam 2012) are not captured by the quarterly CalCOFI sampling frequency.

Deleted: Due to the physical oceanography and variable bathymetry of the SCB, nearshore deep-water areas on the shelf and slope may experience high variability due to localized wind-driven upwelling events (Send and Nam 2012) and mixing from internal waves (Nam and Send 2011). The California Undercurrent transports warm, saline, low-oxygen subtropical water northward along the coast in the SCB and varies seasonally in strength, depth, and direction (Lynn and Simpson 1987), likely contributing to deep-water O_2 variability. ... [1]

Deleted: ,

Deleted: ,

This study focuses on oxygen variability and community composition at depths between 100-400 m along the nearshore environment in the Southern California Bight (SCB). This depth zone is of interest because it encompasses the oxygen limited zone (OLZ) (O_2 < 60 µmol kg^{-1} as defined in Gilly et al. 2013) and supports many important recreational and commercial fish species, including many species of slope rockfish (genus *Sebastes*), which may be vulnerable to deoxygenation (Keller et al. 2015, McClatchie et al. 2010). The OLZ is a transition zone above the oxygen minimum zone (OMZ, O_2 < 22.5 µmol kg^{-1}), where dissolved oxygen levels exclude hypoxia-intolerant species. The shallow upper OMZ boundaries likely experience more temporal variability than lower boundaries because upwelling is a generally shallow phenomenon (< 200 m) and these waters may be more biogeochemically responsive to changes in surface production. Thus, seafloor communities in the OLZ may be highly responsive to short-term and seasonal changes in oxygenation.

Upper slope depths on the US West Coast appear to be especially affected by global trends of oxygen loss (Levin 2018) and long-term trends have been captured by the California Cooperative Oceanic Fisheries Investigations (CalCOFI) quarterly measurements over the past 70 years. Off Monterey Bay in Central California, depths between 100-350 m have seen declines in oxygen of 1.92 µmol kg^{-1} year^{-1} between 1998-2013 (Ren et al. 2018). In the SCB, oxygen declines of 1-2 µmol kg^{-1} year^{-1} have been reported by several studies over a period of ~30 years (Bograd et al. 2008, 2015, McClatchie et al. 2010, Meinvielle and Johnson 2013), with the largest relative changes occurring at 300 m (Bograd et al. 2008). The proposed mechanisms for observed oxygen loss include increased advection of and decreasing oxygen in Pacific Equatorial Water (PEW) (Meinvielle and Johnson 2013, Bograd et al. 2015, Ren et al. 2018) and increased respiration, which is suspected to contribute more to oxygen loss at shallower depths (< 150 m) (Booth et al. 2014, Bograd et al. 2015, Ren et al. 2018). Long-term declines in pH and aragonite saturation state have also been demonstrated for the California Current System over similar periods using ROMS simulations (Hauri et al. 2013). Understanding the superposition of these long-term trends on natural high-frequency variability will be key to evaluating biotic responses.

Despite well documented long-term trends, no published high-frequency deep-water O_2 or pH measurements are available for depths below 100 m in the Southern California Bight (SCB). Notably, daily, weekly and even seasonal low oxygen extreme events (e.g. Send and Nam 2012) are not captured by the quarterly CalCOFI sampling frequency. Due to the physical oceanography and variable bathymetry of the SCB, nearshore deep-water areas on the shelf and slope are thought to experience high variability due to localized wind-driven upwelling events (Send and Nam 2012) and mixing from internal waves (Nam and Send 2011). In addition, the California Undercurrent transports warm, saline, low-oxygen subtropical water northward along the coast in the SCB and varies seasonally in strength, depth, and direction (Lynn and Simpson 1987), likely contributing to deep-water O_2 variability.

The goals of this study were to: (i) increase sensor accessibility to nearshore deep-water ecosystems through the development and testing of a small autonomous Nanolander, (ii) characterize deep-water O_2 variability over hours, days, and weeks at upper slope depths in the SCB relative to mean deoxygenation trends over decades, and identify dominant timescales and depths of variability between 100-400 m, (iii) describe shelf and slope assemblages using the Nanolander camera system,

Deleted: SCB.

Moved (insertion) [3]

Moved up [3]: Off Monterey Bay in Central California, depths between 100-350 m have seen declines in oxygen of 1.92 µmol kg^{-1} year^{-1} between 1998-2013 (Ren et al. 2018). In the SCB, oxygen declines of 1-2 µmol kg^{-1} year^{-1} have been reported by several studies over a period of ~30 years (Bograd et al.

Moved (insertion) [4]

Deleted:).

Moved up [4]: , McClatchie et al. 2010, Meinvielle and Johnson 2013), with the largest relative changes occurring at 300 m (Bograd et al. 2008). The proposed mechanisms for observed oxygen loss include increased advection of and decreasing oxygen in Pacific Equatorial Water (PEW) (Meinvielle and Johnson 2013, Bograd et al. 2015, Ren et al. 2018) and increased respiration, which is suspected to contribute more to oxygen loss at shallower depths (< 150 m) (Booth et al. 2014, Bograd et al. 2015, Ren et al. 2018).

Deleted:

Moved (insertion) [5]

Moved up [5]: been demonstrated for the California Current System over similar periods using ROMS simulations (Hauri et al. 2013).

Deleted: significant

Deleted:

Moved (insertion) [2]

Deleted: are

and (iv) examine if and how the seafloor community responds to O_2 variability at short timescales (daily, weekly, seasonal) in terms of community composition and diversity.

2 Methods

2.1 Nanolander development and deployment

Autonomous landers have been used successfully to observe abyssal and deep-sea trench communities (e.g., Jamieson et al. 2011, Gallo et al. 2015), however, these landers were large and required a ship with an A-frame and winch to deploy and recover. For this study, the goal was to develop a deep-water lander that could easily be hand-deployed out of a small boat and that was capable of continuously collecting hydrographic and fish and invertebrate assemblage data from near the seafloor for several weeks at a time. With this goal in mind, the "Nanolander" *Deep Ocean Vehicle (DOV) BEEBE*, was developed and built (Global Ocean Design, San Diego, CA) (Fig. 1A, Fig. 2). *DOV BEEBE* is named for William Beebe (1877-1962) who illuminated the deep-sea world during his Bathysphere dives (Beebe 1934).

DOV BEEBE stands 1.6 m tall and is 0.36 m wide and 0.36 m deep. When *DOV BEEBE* is deployed, the vertical distance from the base of the Nanolander to the seafloor is ~51 cm (Fig. 1B). This distance is defined by the length of the anchor chain connecting the lander release system to the expendable iron anchor and may be shortened or lengthened. The Nanolander frame is made of marine-grade high-density polyethylene (HDPE) (brand name "Starboard") and reinforced with fiberglass pultruded channel and angle beams for structure, reducing in-water weight. HDPE has a specific gravity of <1, close to neutrally buoyant. The specific gravity of fiberglass is 2/3 that of aluminium, requiring less flotation to achieve neutral buoyancy. Both plastic materials are impervious to saltwater corrosion. Alloy 316 stainless steel fasteners hold the frame together.

Within the frame sit three plastic spheres that are 25.4 cm in diameter; the spheres are made of injection-molded polyamide with 15% glass fibers for additional strength. The novel design aspects of the Nanolander include the use of plastic spheres for both instrument housing and flotation, which allow the vehicle to be smaller and lighter. Previous generation landers, such as the landers used for the *DEEPSEA CHALLENGE* Expedition (Gallo et al. 2015), used syntactic foam for flotation, which is more expensive and requires a metal support frame. While glass spheres have a deeper maximum operational depth (to 11 km), the use of glass-filled polyamide spheres in the Nanolander has machining advantages and decreases the price point. The plastic spheres used for *DOV BEEBE* are pressure-tolerant to 1 km; new spheres with 20% glass content are pressure tolerant to 2 km.

All three main spheres of *DOV BEEBE* are used to support electronics and instrumentation required for deployment, data collection, and recovery. The upper sphere houses an Edgetech BART (Burnwire-Acoustic-Release-Transponder) board, which is the prime means of communication with the Nanolander. A transducer is bonded to the exterior of the upper sphere, positioned to point upwards with a clear view to the surface. The Edgetech BART board has four pre-programmed commands that enable and disable acoustic responses, and initiate the burn command for recovery. An overboard transducer and an

Deleted: at water depths to 1000 m.

Moved down [6]: Alloy 316 stainless steel fasteners hold the frame together.

Deleted: 5.25 ft tall (1.6 m) and is 1.17 ft (36 cm) wide and 1.17 ft (36 cm) deep. The Nanolander frame is made of marine-grade high-density polyethylene (brand name "Starboard") and reinforced with fiberglass pultruded channel and angle beams for structure, reducing in-water weight.

Deleted: Within the frame sit three glass-filled polyamide trawl float spheres that are 10 inches (~25 cm) in diameter. These spheres are used for both buoyancy and instrument housing and are rated to 1000 m. When needed, additional smaller glass-filled polyamide spheres were used to increase buoyancy.

Deleted: 18 inches (~

Deleted:)

Moved (insertion) [6]

Deleted: bounded

Deleted: which

Edgetech deckbox are used to communicate acoustically with the upper sphere, and allow distance ranging on the Nanolander. The battery for the BART board is housed in the upper sphere with the BART board.

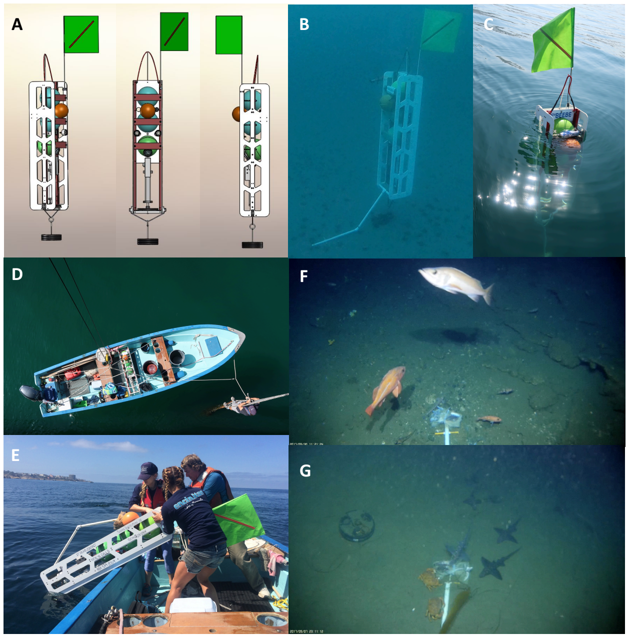

Figure 1: *DOV BEEBE* is an autonomous, hand-deployable Nanolander capable of operating to 1000 m depth. It is outfitted with a Seabird MicroCAT-ODO environmental sensor for collecting high-frequency measurements of near-seafloor temperature, oxygen, salinity, and pressure, and a camera and light system for collecting videos of seafloor communities. (A) Front and side views showing the general design for *DOV BEEBE* (see additional details in Fig. 2). *DOV BEEBE* is shown deployed at 30 m depth in (B), and floating at the surface in (C) prior to recovery. *BEEBE* can easily be deployed and recovered by hand from a small boat by as few as two people (D, E). Examples of the field of view from the *BEEBE* camera system taken from (F) D100-DM-Fall at ~100 m off Del Mar Steeples Reef showing various rockfish species (genus *Sebastes*) and (G) D200-LJ-2 at ~200 m near the Scripps Reserve showing the presence of cancer crabs and chimaeras. The drop arm with the bait bag can be seen in camera field of view.

The middle sphere functions as a "battery pod" and houses the batteries and battery management system (BMS) that power the two external LED lights. The LED lights are powered by a circuit consisting of five components: Battery > BMS > Relay > LED Driver > LED lights. Rechargeable lithium-polymer batteries were used and can be recharged through an external cable and charger system without having to open the middle sphere. For all but one deployment, a 30-ampere hour (Ah) battery stack was used to power the LED lights, which was composed of three 14.8v/10 Ah units. For the last deployment, power

Deleted: power supply
Moved (insertion) [7]
Formatted: Indent: First line: 0.5"
Formatted: Font:12 pt
Formatted: Caption, Indent: First line: 0"
Moved (insertion) [8]
Deleted: circuit engineered to power the
Deleted: consists
Deleted: Battery Management System (
Deleted:)
Deleted: are

capacity was upgraded to 32 Ah by using two 14.8v/16 Ah batteries. In each case, each individual battery (10 or 16 Ah) had its own battery management system (BMS) with a low voltage cut-out (LVCO) to ensure that battery discharge never went below a critical threshold (12.0 v), which would damage the battery. This battery system is novel and was developed specifically to fit within the spatial constraints of the sphere and provide high power capacity.

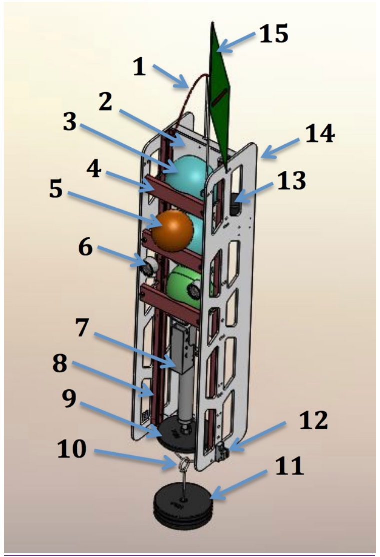

Figure 2: A detailed schematic of the Nanolander *DOV BEEBE* components: 1) Spectra lifting bale; 2) High-density polyethylene (HDPE) centerplate; 3) ~25 cm polyamide spheres stacked top, middle and bottom, see description, Section 2.1; 4) sphere retainer; 5) auxiliary ~18 cm flotation sphere; 6) oil-filled LED lights; 7) Seabird MicroCAT-ODO in the lower payload bay; 8) central fiberglass frame; 9) stabilizing counterweight; 10) anchor slip ring; 11) expendable iron anchor (bar bell weights); 12) burnwire release and mount, one port side, one starboard side; 13) Edgetech hydrophone for acoustic command and tracking; 14) HDPE side panels; and 15) surface recovery flag. Not shown: drop arm on front (see Fig. 1B and 1E).

Formatted: Caption, Indent: First line: 0"

Formatted: English (UK)

The relay and LED drivers are contained within the lower sphere, which houses all components of the camera system, and includes the viewport. The camera system uses a Mobius Action Camera with a time-lapse assembly, which was modified by Ronan Gray (SubAqua Imaging Systems, San Diego, CA) and William Hagey (Pisces Design, La Jolla, CA). The SphereCam manual is provided as Supplement 1A. The camera system has 14 different time-lapse options, including continuous video, time-lapse images, and time-lapse video at pre-programmed intervals. For these deployments, a sampling interval of 20 seconds of video every 20 minutes was used. A sealed magnetic switch triggers the camera system to begin programmed sampling at a pre-determined interval. An internal light-sensitive relay, pointed towards a camera indicator LED,

Deleted:

triggers the external LED lights to power on. The two LED lights are attached to the body of the Nanolander and positioned on either side of the middle sphere. All spheres were sealed with a Deck Purge Box (Global Ocean Design, San Diego, CA) using a desiccant cartridge to remove moisture, and were held together by a vacuum of ~7 psi (~1/2 atm).

Below the bottom camera sphere, *DOV BEEBE* has a mounted SBE 37-SMP-ODO instrument (Sea-Bird Scientific) with titanium housing, rated to 7000 m. The MicroCAT CT(D)-DO is a highly accurate sensor designed for moorings and other long-duration, fixed-site deployments. It includes a conductivity, temperature, pressure, and SBE 63 optical dissolved oxygen sensor. Initial sensor accuracy is +/- 3.0 μmol kg^{-1} for oxygen measurements, +/- 0.1% for pressure measurements, +/- 0.002°C for temperature measurements, and +/- 0.0003 S m^{-1} for conductivity measurements, and drift is minimal. The SBE MicroCAT was programmed to take samples every five minutes for the length of the whole deployment.

A drop-arm is mounted on the front of *DOV BEEBE*, and is secured with a release during deployment. Initially a galvanic release was used, but a stack of 3-4 "Wint O Green" lifesavers was found to be more time-efficient. The drop-arm served three functions: it stabilized the Nanolander when exposed to current, it had a ~15 cm cross-bar for visual sizing reference, and it was used to attach bait for each deployment. The bait used was composed of an assortment of previously frozen demersal fishes that are part of the SCB upper margin demersal fish community. Bait was secured within a mesh cantaloupe bag and secured to the drop-arm with Zip-Ties for each deployment. All bait had been eaten by recovery.

DOV BEEBE is positively buoyant in water, and is deployed with ~18 kg of sacrificial iron weights. The weights are attached by a sliding link onto a metal chain, which is secured on each side to the base of the Nanolander using a burn wire (Fig. 2). Successful release of either burn wire allows the metal link to slide off the chain and drop the weights, releasing the Nanolander from the bottom. *DOV BEEBE*'s estimated descent rate is ~100 m per minute, and ascent rate is ~60 m per minute, following release of the weights. Once at the surface, *DOV BEEBE* floats ~0.45 m above the water and has a large flag, which assists with visual detection of the Nanolander (Fig. 1C). In addition to the three main spheres, additional smaller spheres were used, as needed, to increase buoyancy (Fig. 2).

Seven deployments were conducted during the study period, ranging from 15-35 days, and at targeted depths of 100-400 m (Table 1). Two early deployments (D200-LJ-1 and D200-LJ-2) were done near the Scripps Reserve off La Jolla, CA and five subsequent deployments (D100-DM-Fall, D200-DM, D300-DM, D400-DM, D100-DM-Spr) targeted a nearby rockfish habitat – the Del Mar Steeples Reef, CA (Fig. 3). Despite relatively close spatial proximity (~10 km), the local bathymetry differed between the LJ and DM deployments (Fig. 3); the LJ deployments were close to a submarine canyon feature, while the DM deployments were on a gradually sloping margin. Environmental and camera-based community data were collected during six of the seven deployments; only environmental data are available from the first deployment (D200-LJ-1) due to a camera technical problem. We aimed to conduct repeat deployments at each site to capture seasonal differences between a period of relaxed upwelling (fall/winter) and a period of strong upwelling (spring/summer), however full sampling was not feasible due to time and equipment constraints. Consequently, only one repeat deployment is available for ~100 m at Del Mar Steeples Reef (D100-DM-Fall and D100-DM-Spr).

Deleted: 12
Deleted: .
Deleted: housed within a
Deleted: and
Deleted: 5
Deleted: in
Deleted: 6 inch (
Deleted: .24
Deleted:)
Deleted: 40 lbs
Deleted: .
Deleted: 1.5 feet (
Deleted:)
Deleted: .

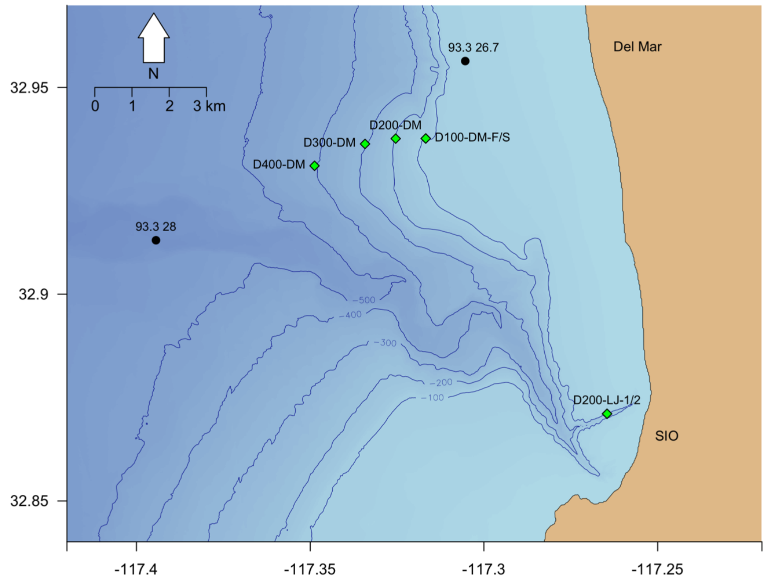

Figure 3: Map of Nanolander *DOV BEEBE* deployments shown in relation to local bathymetry and nearby stations sampled quarterly by the California Cooperative Oceanic Fisheries Investigations (CalCOFI). Green diamonds indicate Nanolander deployments, black circles indicate CalCOFI stations with station labels, and isobaths show 100, 200, 300, 400, and 500 m depth contours. Note that green diamonds labelled as D200-LJ-1/2 and D100-DM-F/S represent two deployments each, but points overlap due to proximity.

2.2 Characterizing environmental variability on the shelf and upper slope

Upon recovery of the Nanolander, time-series data from the MicroCAT were analyzed to assess how environmental variability (O_2, T, salinity) changes with depth. Since partial pressure of oxygen may be more biologically meaningful than oxygen concentration for understanding animal exposures to oxygen, we also calculated oxygen partial pressure as in Hofmann et al. (2011a). Oxygen and pH naturally co-vary along the continental margin driven by respiration. To examine variability of carbonate chemistry parameters, pH, Ω_{arag}, and Ω_{calc} were estimated using empirical equations derived for this

Formatted: Indent: First line: 0.5"

Moved up [7]:

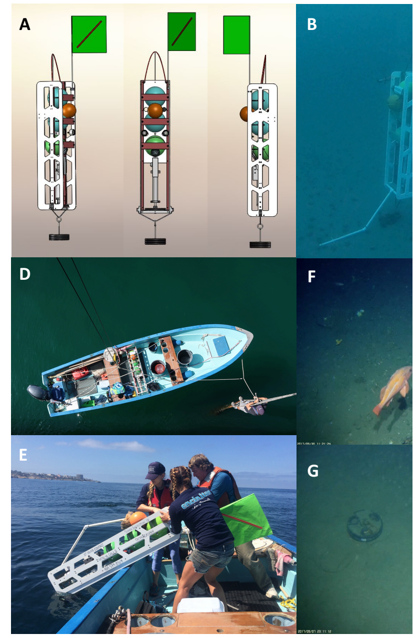

Figure 1: ***DOV BEEBE*** **is an autonomous, hand-deployable Nanolander capable of operating to 1000 m depth. It is outfitted with a Seabird MicroCAT-ODO environmental sensor for collecting high-frequency measurements of near-seafloor temperature, oxygen, salinity, and pressure, and a camera and light system for collecting videos of seafloor communities.**

Formatted: Font:12 pt

Formatted: Heading 2

Deleted: **The design for** ***DOV BEEBE*** **is shown in (A), and**

Moved up [8]: ***DOV BEEBE*** **is shown deployed at 30 m depth in (B), and floating at the surface in (C) prior to recovery.**

Formatted: English (UK)

Deleted: ***BEEBE*** **can easily be deployed by several people from a small boat (D, E). Examples of the field of view from the camera system are shown in (F) from D100-DM-Fall at ~100 m off Del Mar Steeples Reef and in (G) from D200-LJ-2 at ~** ... [2]

Formatted: Left

Deleted: high-frequency

region in Alin et al. (2012). Ω_{arag}, and Ω_{calc} are the calcium carbonate saturation state of aragonite and calcite respectively, and conditions favor calcium carbonate dissolution when $\Omega < 1$.

The mean and ranges of environmental conditions were compared across depths and deployments to characterize differences in environmental variability that seafloor communities were exposed to over short timescales. Probability density distributions of environmental conditions were used to visualize differences in environmental conditions for each deployment. The coefficient of variation (CV) (i.e. the ratio of the standard deviation to the mean) was calculated for environmental variables for each deployment as a standardized measure of dispersion and compared across deployments and depths. Additionally, the percent of measurements in which conditions were hypoxic (O_2 < 60 µmol kg^{-1}), severely hypoxic (O_2 < 22.5 µmol kg^{-1}), or undersaturated with respect to aragonite ($\Omega_{arag} < 1$) or calcite ($\Omega_{calc} < 1$) was determined for each deployment.

Table 1: Information for seven deployments conducted with the Nanolander *DOV BEEBE* including deployment dates, length, location, depth, environmental conditions for each deployment, total number of 20-second video samples available for the community analysis, and camera and light performance for each data deployment. [O_2] < 60 µmol kg^{-1} is defined as hypoxic, [O_2] < 22.5 µmol kg^{-1} is defined as severely hypoxic, and Ω_{arag} ≤ 1 and Ω_{calc} ≤ 1 are defined as undersaturated with respect to aragonite or calcite, respectively. Mean and range O_2 percent saturation and pO_2 (kPa) for each deployment are provided in Supplement 1B. CV = coefficient of variation (i.e. the ratio of the standard deviation to the mean). pH_{est} is estimated pH, calculated using empirical relationships from Alin et al. (2012).

Deleted: are

Deleted: time-scales

Moved (insertion) [9]

Formatted: Indent: First line: 0"

Moved (insertion) [10]

	D200-LJ-1	D200-LJ-2	D100-DM-Fall	D200-DM	D300-DM	D400-DM	D100-DM-Spr
Dates	Aug 17-Sep 1, 2017	Sep 7-Sep 25, 2017	Sep 29-Nov 3, 2017	Nov 9-29, 2017	Dec 12, 2017 - Jan 5, 2018	Jan 23-Feb 8, 2018	Mar 8-Mar 29, 2018
Deployment Length	~15 days	~19 days	~35 days	~20 days	~24 days	~16 days	~21 days
Location	Scripps Coastal Reserve (32.87108° N, 117.26459° W)	Scripps Coastal Reserve (32.87108° N, 117.26457° W)	Del Mar Steeples Reef (32.93765° N, 117.31675° W)	Del Mar Steeples Reef (32.93762° N, 117.3254° W)	Del Mar Steeples Reef (32.93633°N, 117.33422°W)	Del Mar Steeples Reef (32.93105°N, 117.34875°W)	Del Mar Steeples Reef (32.93765°N, 117.31675°W)
Bottom Depth (m)	179	178	99	192	295	399	98
Mean Temp (°C)	10.07	9.88	11.10	9.51	8.39	7.42	9.80
Temp Range (°C)	9.72-10.43	9.45-10.44	10.35-12.26	8.94-10.21	7.99-8.77	6.97-7.89	9.39-10.30
CV Temp (%)	1.35	1.69	2.89	2.11	1.88	2.02	1.70
Mean $[O_2]$ (µmol kg^{-1})	70.75	77.61	132.00	82.10	49.38	28.97	103.95
$[O_2]$ range (µmol kg^{-1})	48.82-103.87	49.41-108.26	110.40-156.50	63.33-102.96	39.89-59.36	21.19-38.41	91.22-123.01
CV $[O_2]$ (%)	13.72	12.92	5.07	9.82	7.02	10.20	5.72
Mean pHest	7.646	7.655	7.759	7.658	7.594	7.553	7.70
pHest Range	7.607-7.704	7.605-7.711	7.713-7.814	7.625-7.699	7.575-7.613	7.538-7.572	7.671-7.732
CV pHest (%)	0.22	0.23	0.2	0.19	0.09	0.08	0.15
Conditions hypoxic (% time)	12.64%	1.88%	0%	0%	100%	100%	0%
Conditions severely hypoxic (% time)	0%	0%	0%	0%	0%	1.12%	0%
Conditions undersaturated (aragonite) (% time)	99.65%	99.77%	0%	100%	100%	100%	92.80%
Conditions undersaturated (calcite) (% time)	0%	0%	0%	0%	0%	97.30%	0%
Number of 20-sec video samples for analysis	N/A	1009	876	1012	406	594	396
Number of video samples with good visibility	N/A	1009	876	656	6	594	396
Amount of time before lights first failed (h)	N/A	5.61	4.77	5.63	2.26	3.30	2.21

Previous studies have found that changes in oxygen and pH in the Southern California Bight are associated with changes in the volume of Pacific Equatorial Water (PEW) transported in the California Undercurrent (Bograd et al. 2015, Nam et al. 2015). PEW is characterized by low oxygen, warm, high salinity conditions, and is composed of two water masses, the 13°C water mass (13CW) and the deeper Northern Equatorial Pacific Intermediate Water Mass (NEPIW) (Evans et al. 2020). Spiciness, the degree to which water is warm and salty, is a state variable that is conserved along isopycnal surfaces (Flament 2002) and can be used as a tracer for PEW (Nam et al. 2015). We calculated spiciness using the “oce” R package (Kelley and Richards 2017) and examined how oxygen concentration varies with temperature and spiciness across depths and deployments. Spiciness is used to examine differences in spatial variation between water masses, which otherwise may not be apparent using isopycnal surfaces because the effects of warm temperature and high salinity cancel each other out. “Spicier” water is warmer and saltier.

Formatted: Font:12 pt

Deleted: and

Deleted: .

Deleted: which

Deleted:),

To identify the dominant timescale of variability for oxygen, a spectral analysis was conducted as in Frieder et al. (2012) on the oxygen time series for each deployment. To look at diurnal and semidiurnal patterns, one day was used as the unit of time, and the number of observations based on the sampling frequency, was 288. Spectral analyses were conducted on a detrended time series using a fast fourier transform. Results were displayed using a periodogram and the period of the dominant signal was compared across deployments. The oxygen time series for each deployment was also decomposed using the "stats" package (R Core Team 2019) to look at the trend, daily, and random signals that contribute to the overall data patterns.

2.3 Short-term oxygen variability in the context of longer trends

To examine O_2 variability over shorter (i.e. daily and weekly) timescales compared to longer (i.e. seasonal, interannual, multidecadal) timescales, we compared our Nanolander results with the annual rates of oxygen loss reported for the SCB nearshore region (Bograd et al. 2008) as well as CTD casts from nearby CalCOFI station 93.3 28 (Fig. 3). CalCOFI station 93.3 26.7 was also nearby, but was too shallow for comparison with the Nanolander deployments (Fig. 3). Quality controlled CTD casts from station 93.3 28 were available for a ~16-year period (Oct 2003-November 2019), representing data from 61 cruises (calcofi.org). CTD data were used to examine characteristics of variability of temperature and oxygen through the water column, including mean conditions, the standard deviation, and the coefficient of variation across the 16-year period of quarterly samples. Oxygen data at 100, 200, 300, and 400 m were extracted to compare the distribution of observations across this 16-year period with the high-frequency measurements from the ~3-week Nanolander deployments. Additionally, we tested for significant linear trends in temperature or oxygen at 100, 200, 300, and 400 m, to examine recent (2003-2019) warming and deoxygenation trends at the CalCOFI station closest to the Nanolander deployments.

2.4 Assessing community responses to oxygen variability

Video segments recorded by the camera system were annotated to analyze if and how seafloor communities differ with respect to environmental conditions. A total of 4,293 20-second video segments were collected and annotated in total. For each 20-second video, both invertebrates and vertebrates within the frame of view were identified to lowest taxonomic level and counted.

Since visibility was impaired during certain deployments due to high turbidity, each video clip was categorized by visibility quality using the following categories: 1 (can see the bottom, good visibility), 2 (can only see the drop-arm, poor visibility), or 3 (drop-arm can no longer be seen, no visibility). Only samples with a visibility category of 1 were utilized in subsequent community analyses so that differences in community patterns were not due to differences in visibility.

Deleted: 2.3

Deleted:

Formatted: Indent: First line: 0"

Moved up [9]: **Table 1: Information for seven deployments conducted with the Nanolander *DOV BEEBE* including deployment dates, length, location, depth, environmental conditions for each deployment, total number of 20-second video samples available for the community analysis, and camera and light performance for each data deployment. $[O_2] < 60$ µmol kg^{-1} is defined as hypoxic, $[O_2] < 22.5$ µmol kg^{-1} is defined as severely hypoxic, and $\Omega_{arag} < 1$ and $\Omega_{calc} < 1$ are defined as undersaturated with respect to aragonite or calcite, respectively. Mean and range O_2 percent saturation and pO_2 (kPa) for each deployment are provided in Supplement**

Deleted:

Deleted: 1D.

Moved up [10]: **CV = coefficient of variation (i.e. the ratio of the standard deviation to the mean). pH_{est} is estimated pH, calculated using empirical relationships from Alin et al. (2012).**

Non-metric multidimensional scaling was used to assess community-level differences across deployments. The R package "vegan" (Oksanen et al. 2017) was used for nMDS analysis and a Wisconsin double standardization was performed and counts were transformed using a square-root transformation. These standardizations are frequently used when working with datasets with high-count values and have been found to improve nMDS results (Oksanen et al. 2017). Bray-Curtis dissimilarity was used as the input and community dissimilarities were mapped onto ordination space for the nMDS analysis. Rare species (<8 observations across all deployment samples) and video samples with only one animal observation were removed from the community matrix, resulting in a total number of 3357 video samples and 43 unique species included in the community analysis.

Since fishes are typically less hypoxia-tolerant than invertebrates (Vaquer-Sunyer and Duarte 2008), we hypothesized there would be a shift from a fish- to an invertebrate-dominated seafloor community that correlated with decreasing oxygen conditions. Samples from all deployments were categorized as "Fish Dominant", "Equal", or "Invertebrate Dominant" based on if there were more fishes or more invertebrates observed in each 20-second video sample. These categories were then projected onto ordination space and superimposed with oxygen contours using the ordisurf function in "vegan".

Since low oxygen conditions have been found to depress fish diversity (Gallo and Levin 2016), fish species accumulation curves relative to the number of video samples were examined to look at differences in fish diversity across deployments. We selected this metric of diversity since the number of video samples differed across deployments (Table 1). Only video samples in which fish were present were included in the calculation of the species accumulation curves. A table of all fish species observed during the deployments is included in Supplement 1C.

To test the ability of the Nanolander to capture short-term responses in seafloor communities, we selected two deployments that had high environmental variability (D200-LJ-2 and D200-DM). For these deployments, samples were grouped in day (6:00 am-5:59 pm PST) and night (6:00 pm-5:59 am PST) categories and oxygen categories ("High", "Intermediate", and "Low"). Oxygen categories were determined separately for each deployment based on the deployment time series, and were selected to showcase extremes: "High" samples represented the highest 10% of observed oxygen conditions, and "Low" samples the lowest 10% of observed oxygen conditions for the deployment. All other samples were categorized as "Intermediate." An nMDS analysis was performed to look at differences in communities in relation to diurnal patterns and oxygen conditions within the timeframe of a single deployment. Rare species with fewer than three observations across the deployment time series were removed from the community matrices, resulting in a community matrix with 844 video samples and 19 species for D200-LJ-1 and 645 video samples and 17 species for D200-DM. These were used in the nMDS analysis.

	D200-LJ-1	D200-LJ
Dates	Aug 17-Sep 1, 2017	Sep 7-Sep 2017
Deployment Length	~15 days	~19 day
Location	Scripps Coastal Reserve (32.87108° N, 117.26459° W)	Scripps Co Reserve (32.87108 117.26457
Bottom Depth (m)	179	178
Mean Temp (°C)	10.07	9.88
Temp Range (°C)	9.72-10.43	9.45-10.
CV Temp (%)	1.35	1.69
Mean [O_2] (µmol kg^{-1})	70.75	77.61
[O_2] range (µmol kg^{-1})	48.82-103.87	49.41-108
CV [O_2] (%)	13.72	12.92
Mean pHest	7.646	7.655
pHest Range	7.607-7.704	7.605-7.7
CV pHest (%)	0.22	0.23
Conditions hypoxic (% time)	12.64%	1.88%
Conditions severely hypoxic (% time)	0%	0%
Conditions undersaturated (aragonite) (% time)	99.65%	99.77%
Conditions undersaturated (calcite) (% time)	0%	0%
Number of 20-sec video samples for analysis	N/A	1009
Number of video samples with good visibility	N/A	1009
Amount of time before lights first failed (h)	N/A	5.61

Deleted:

Formatted: Font:12 pt

Deleted:

Deleted: Dominated

Deleted: rarefaction diversity and

Deleted: rarefaction

Deleted: 3

3 Results

3.1 Nanolander performance

DOV BEEBE was found to be a reliable platform for deployment, recovery, and data collection. Small boats were used for deployment and recovery (Fig. 1D and E) and *DOV BEEBE* was easily transported by lab cart or car. The Nanolander framework was robust and showed very few signs of wear following multiple deployments. Spheres showed no signs of leakage or vacuum loss, and acoustic communication worked well during all deployments.

Memory and power capacity often limit deployment times for long-term, deep-sea deployments. In this study, the main technological limitation we ran into was limited battery capacity to power the LED lights. As opposed to 8 hours of estimated LED performance time, field performance ranged from 2.2 to 6.6 hours total time, which meant that the total time of biological data collection was shortened and ranged from 5.5 to 16.5 days, respectively (Table 1). Memory and power were not issues for the camera system; the 128 GB micro SD card was cleared and the battery pack was fully recharged following each deployment. Video quality was high enough to allow species-level identifications and the light from the LEDs was sufficient to light the field of view (Fig. 1F and G). The SeaBird MicroCAT-ODO also performed without any issues and had sufficient battery and memory capacity for all deployments. If not for power limitations to the LED lights, the camera system and SBE MicroCAT would have allowed for longer sampling (~1 month and potentially longer). The basic Nanolander itself can stay *in situ* for up to two years. Detailed descriptions of Nanolander performance can be found in Gallo (2018).

3.2 Characteristics and drivers of oxygen variability across short time-scales

Natural variability of environmental parameters was assessed from time series data collected during each deployment and compared across depths (100, 200, 300, and 400 m), and season (fall compared to spring). Means and ranges for temperature, oxygen, salinity, and pH_{est} for each deployment were determined (Table 1). At ~100 m, conditions were never hypoxic (i.e. < 60 µmol kg^{-1}), although the mean oxygen concentration was significantly lower during the spring upwelling season deployment (D100-DM-Spr, mean O_2 = 104 µmol kg^{-1}), compared to the fall deployment when upwelling was relaxed (D100-DM-Fall, mean O_2 = 132 µmol kg^{-1}) (ANOVA, $p < 0.001$). pH_{est} was also lower during the spring deployment (D100-DM-Spr, mean pH_{est} = 7.696) than during the fall deployment at ~100 m (D100-DM-Fall, mean pH_{est} = 7.759) (ANOVA, $p < 0.001$), and temperatures were on average 1.3°C colder, consistent with upwelling conditions (Table 1, Fig. 4). While conditions were never undersaturated with respect to aragonite ($\Omega_{arag} < 1$) during the fall deployment, during the spring deployment, conditions were undersaturated ~93% of the time (Table 1).

At ~200 m, hypoxic conditions (O_2 < 60 µmol kg^{-1}) were encountered, however conditions were only hypoxic for relatively short portions of the deployment (~13% for D200-LJ-1, ~2% for D200-LJ-2, and never hypoxic for D200-DM) (Table 1). Conditions were almost always undersaturated with respect to aragonite ($\Omega_{arag} < 1$) (Table 1). At ~300 m (D300-DM) and ~400 m (D400-DM), mean temperatures were colder than shallower depths, and mean oxygen and pH_{est} conditions were lower than shallower depths (Table 1, Fig. 4). At both 300 and 400 m, conditions were continuously hypoxic, and at 400

Deleted: We found that

Deleted: to deployment duration

Deleted: the

Deleted: requirement for

Formatted: English (UK)

Deleted: 2

Deleted: These results, if characteristic of other years, suggest that at depths around 200 m, benthic organisms are periodically exposed to hypoxic conditions in the late summer and fall, but these conditions are not continuous.

Deleted:

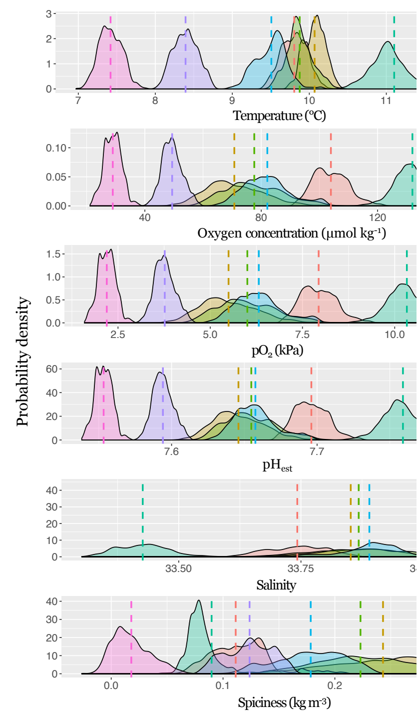

Deleted: 2

Deleted: depths

m (D400-DM) conditions were severely hypoxic (i.e. O_2 < 22.5 µmol kg^{-1}) for ~1% of the time-series (Table 1). Both D300-DM and D400-DM were conducted during the fall/winter, when upwelling conditions are relaxed, therefore deployments likely captured the less extreme (higher oxygen, higher pH) conditions. At ~300 m, conditions were undersaturated with respect to aragonite (Ω_{arag} < 1) but not calcite, whereas at ~400 m, conditions were also undersaturated with respect to calcite (Ω_{calc} < 1) for most of the deployment (Table 1).

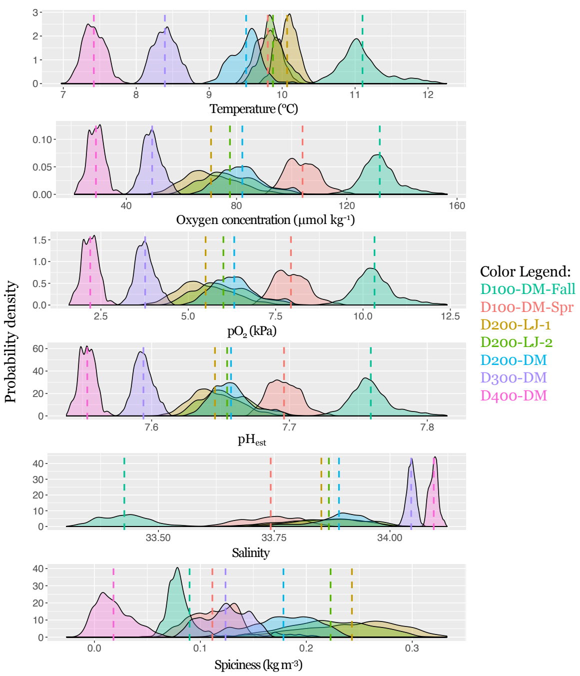

Figure 4: Mean and variance of near-seafloor temperature, oxygen concentration, oxygen partial pressure, pH_{est}, salinity, and spiciness. The probability density of data collected for each deployment is shown, with the color of the data distributions corresponding to each deployment (as indicated in the color legend). The mean is indicated with a dotted line in the same color and exact values are given in Table 1. pH_{est} is estimated pH, calculated using empirical relationships from Alin et al. (2012). Sampling dates for each deployment are given in Table 1.

While we expected that O_2 variability would decrease with depth, instead we found that the greatest variability in oxygen conditions over these short time-scales was observed at ~200 m (Table 1). All three deployments from ~200 m showed broad probability density distributions of environmental conditions (Fig. 4) and large ranges in oxygen and pH_{est} for the

Deleted: This suggests that at ~300 m, seafloor communities are continuously exposed to hypoxic conditions throughout the year, and at ~400 m communities are periodically exposed to OMZ conditions. At ~300 m, the seawater is

Deleted: are

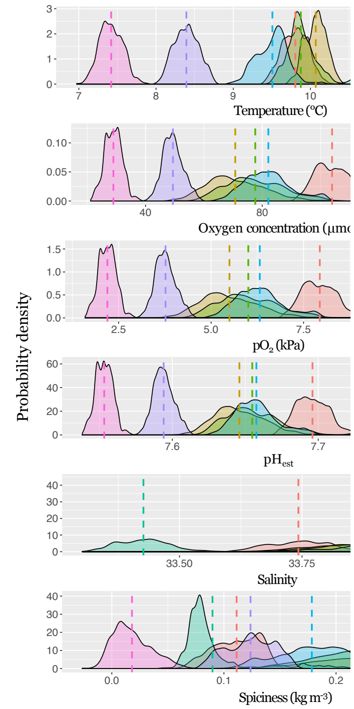

Deleted:

Formatted: Font:12 pt

Formatted: Font:12 pt

Deleted: 2:

Formatted: Subscript

Formatted: English (US)

Formatted: Indent: First line: 0"

Deleted: variance

Deleted: 2

deployment period (Table 1). The average daily range in oxygen concentration (i.e. daily maximum-daily minimum) was highest for D200-LJ-2 (~34 µmol kg^{-1}), followed by D200-LJ-1 (~31 µmol kg^{-1}), followed by D200-DM (~24 µmol kg^{-1}). The average daily oxygen range for both ~100 m deployments was lower (~20 µmol kg^{-1} for D100-DM-Fall and ~14 µmol kg^{-1} for D100-DM-Spr). The coefficient of variation (CV) for oxygen at ~200 m was twice higher than for the ~100 m deployments (Table 1). While deployments at ~300 m (D300-DM) and ~400 m (D400-DM) had much narrower probability density distributions of environmental conditions (Fig. 4), the ranges in oxygen and pH_{est} at ~400 m were only slightly smaller than at ~300 m (Table 1). The CV for oxygen was higher at ~400 m (10.20%) compared to ~300 m (7.02%) (Table 1). The average daily range in oxygen concentration was ~11 µmol kg^{-1} for D300-DM and ~8 µmol kg^{-1} for D400-DM. Temperature did not exhibit the same pattern of variability as oxygen, with the highest variability (CV) observed during D100-DM-Fall (~100 m) (Table 1). Variability in pH_{est} (CV) was almost twice higher at shallower depths (< 200 m), than at ~300 or ~400 m (Table 1).

Using a spectral analysis, we found that the dominant frequency underlying oxygen variability for all deployments was close to the semidiurnal tidal period (~12.4 hrs) (Supplement 1D). When the time series were decomposed into their additive components (i.e. daily trend, underlying trend, and random noise), time series for all depths showed a clear diurnal and semi-diurnal signal (Supplement 1E). Thus, oxygen variability on the outer shelf and upper slope is mainly driven by tides. The relative amplitude of the dominant signal in the periodogram decreases with increasing depth, suggesting that the strength of the tidal signal weakens with depth. Oxygen conditions tend to increase during ebb tide as the tide retreats, and decrease during flood tide as the tide rises (Supplement 1F). Oxygen variability does not appear to increase with tidal amplitude; for D100-DM-Spr, D200-LJ-1, and D200-LJ-2 the daily oxygen range appears to be negatively correlated with the daily tidal range (Supplement 1F).

Oxygen concentration was found to be significantly positively correlated with temperature for all deployments (LR, $p < 0.001$), however, the explanatory power of the regressions differed across depths (100, 200, 300, and 400 m) and the slopes of the regressions differed between locations (Scripps Reserve and Del Mar Steeples Reef). At depths deeper than 200 m, there was less variance around the linear trend in oxygen. The highest amount of oxygen variance explained by the linear regression with temperature was found for D400-DM (~400 m, $R^2 = 0.90$), and the lowest amount for D200-DM (~200 m, $R^2 = 0.41$). The two deployments conducted near the Scripps Reserve (D200-LJ-1 and D200-LJ-2) had steeper slopes (Fig. 5) than deployments on the Del Mar Steeples Reef (D100-DM-Fall, D200-DM, D300-DM, D400-DM, D100-DM-Spr), which may be related to bathymetric differences of the sites. Deployments near the Scripps Reserve were in a narrow, deep tendril of the Scripps canyon system, which is surrounded by shallower bathymetry, while the Del Mar deployments were on a gradually sloping margin (Fig. 3).

Oxygen was significantly correlated with spiciness for all deployments (LR, $p < 0.001$), however, the slopes and explanatory power of this relationship differed across depths (100, 200, 300, and 400 m) and season (fall and spring) (Fig. 5). D100-DM-Fall and D100-DM-Spr were conducted at the same location at ~100 m, but during fall and spring, respectively, and exhibited differing relationships between oxygen and spiciness (Fig. 5). In the fall, the relationship between spiciness and

Deleted: 2

Deleted: variance

Deleted: Variance

Deleted: 1A). Deconstructed

Deleted: also

Deleted: at all depths

Deleted: 1B

Deleted: 1C

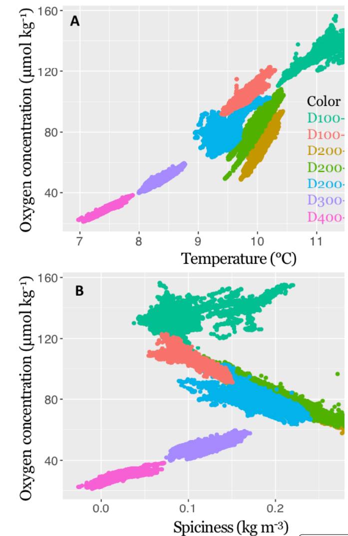

Deleted: ... [3]

Formatted: Font:12 pt

Formatted: Normal, Space After: 10 pt

Moved down [11]: **Data points represent samples taken every five minutes with the SBE MicroCAT-ODO sensor during the seven deployments. Deployments are distinguished by color, as indicated in the color legend. Sampling dates for each deployment are given in Table 1.**

Formatted: Font:9 pt, Bold

Deleted: 3

Deleted: .

Deleted: 3

Deleted: 3

oxygen at ~100 m was weak and positive with low explanatory power ($R^2 = 0.31$). In contrast, during spring, dissolved oxygen was negatively correlated with spiciness, and the linear fit had high explanatory power ($R^2 = 0.81$). At ~200 m (D200-LJ-1, D200-LJ-2, D200-DM), spiciness and oxygen concentration were also negatively correlated, with high explanatory power for the linear fits ($R^2 = 0.98$, 0.92, and 0.61, respectively) (Fig. 5). At deeper depths (~300 and 400 m), the relationship between spiciness and oxygen was significant (LR, $p < 0.001$), but the correlation was positive with high explanatory power of the linear fit (D300-DM $R^2 = 0.61$, D400-DM $R^2 = 0.68$).

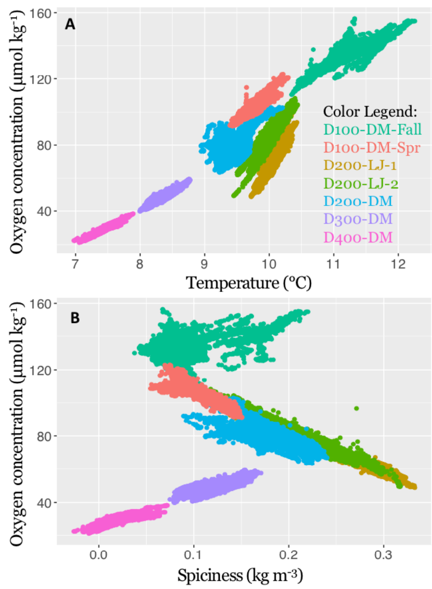

Figure 5: 2017-2018 near-bottom dissolved oxygen concentration in the Southern California Bight shown in relation to temperature (A) and spiciness (B). Data points represent samples taken every five minutes with the SBE MicroCAT-ODO sensor during the seven deployments. Deployments are distinguished by color, as indicated in the color legend. Sampling dates for each deployment are given in Table 1.

3.3 Seafloor community differences and relationship to oxygen conditions

Community data were collected using the camera system during six deployments (Table 1), representing a total of 4,293 20-second videos that were annotated for organismal observations. Unexpected differences in visibility were observed across deployments. Clear conditions were present for deployments D200-LJ-2, D100-DM-Fall, D400-DM and D100-DM-Spr. During D200-DM at Del Mar Steeples Reef, visibility deteriorated throughout the deployment. The following deployment,

Deleted: 3

Formatted: Font:12 pt

Formatted: Normal, Space After: 10 pt

Moved (insertion) [11]

Formatted: Font:9 pt, Bold

D300-DM, which was at ~300 m at Del Mar Steeples Reef, had very poor visibility. For D300-DM, less than 2% of samples had good visibility, 78% had impaired visibility, and 20% had severely impaired visibility due to high sediment turbidity.

The community at the Del Mar Steeples Reef at ~100 m (D100-DM-Fall and D100-DM-Spr) was characterized by high numbers of rockfish (*Sebastes spp.),* especially halfbanded rockfish (*S. semicinctus*), but also included less-observed rockfish species such as the flag rockfish (*S. rubrivinctus*), bocaccio (*S. paucispinis*), rosy rockfish (*S. rosaceus*), and greenstriped rockfish (*S. elongatus*). Other commonly-observed fishes included the pink seaperch, *Zalembius rosaceus*, combfish, *Zaniolepis spp.,* and the spotted cusk-eel, *Chilara taylori*. Invertebrates were not abundant, but included an unidentified gastropod, the tuna crab, *Pleuroncodes planipes*, a yellow coral, as well as others. Except for the singular yellow coral, all other invertebrates were mobile. Seafloor communities for D100-DM-Fall and D100-DM-Spr were very similar, but were distinct from most other deployments (Fig. 6A).

Deployments D200-LJ-2 and D200-DM were in different locations (Table 1, Fig. 3), and the communities observed were very different (Fig. 6A) despite similar depth and environmental conditions (Fig. 4). Soft sediment characterized the benthos at both sites, but D200-LJ-2 was near a submarine canyon, while D200-DM was on a gradually sloping margin (Fig. 3). The community at D200-LJ-2 included eelpouts (*Lycodes spp.),* spotted cusk-eels (*C. taylori*), California lizardfish (*Synodus lucioceps*), and crabs (*Cancer spp.*), as well as, more typical deep-water species such as Dover sole (*Microstomus pacificus*), spotted ratfish (*Hydrolagus colliei*), and dogface witch eels (*Facciolella equatorialis*). In contrast, rockfish (*Sebastes spp*.), combfishes (*Zaniolepis spp*.), and Pacific sanddab (*Citharichthys sordidus*) were commonly observed during D200-DM, and the community was dominated by tuna crabs (*P. planipes*) and pink urchins (*Strongylocentrotus fragilis*) which were present in high abundances. Conversely, during D200-LJ-2, no pink urchins were observed, and tuna crabs were less abundant. Spot prawns (*Pandalus platyceros*) were common community members observed during both D200-LJ-2 and D200-DM, but were not observed during any other deployments.

Only one deployment was conducted at each of the two deeper depths (~300 m and 400 m), and both deployments were near the Del Mar Steeples Reef. Due to high turbidity, the bottom was only visible in a few samples from D300-DM. From these, it appeared that the community was dominated by tuna crabs (*P. planipes*) and pink urchins (*S. fragilis*), though in lower abundances than at D200-DM. Fish were rarely observed, but included Pacific hake (*Merluccius productus*), rockfish (*Sebastes spp.*), Pacific hagfish (*Eptatretus stoutii*), and hundred-fathom codling (*Physiculus rastrelliger*). D300-DM showed similarity to seafloor communities observed during D200-DM and D400-DM (Fig. 6A).

D400-DM represented the deepest deployment (~400 m) and had excellent visibility. The community was dominated by pink urchins (*S. fragilis*), but these were present in lower abundances than at D200-DM. Low numbers of tuna crabs (*P. planipes*) were also present. Fish were rare, but the fishes most commonly observed were Pacific hagfish (*E. stoutii*), blacktip poacher (*Xeneretmus latifrons*), dogface witch eels (*F. equatorialis*), Dover sole (*M. pacificus*), and shortspine thornyhead (*Sebastolobus alascanus*). Both fish and invertebrates were less active and showed less movement in D400-DM than at shallower deployments.

Deleted: rarer
Deleted: Bocaccio
Deleted: surfperch
Deleted: show high similarity
Deleted: are
Deleted: 4A
Deleted: the
Deleted: 4A
Deleted: chimaeras
Deleted: -
Deleted: *Faciolella*
Deleted: combfish
Deleted: *S.*
Deleted: In contrast
Deleted: each
Deleted:)
Deleted: poor visibility
Deleted: *E.*
Deleted: 4A
Deleted: common

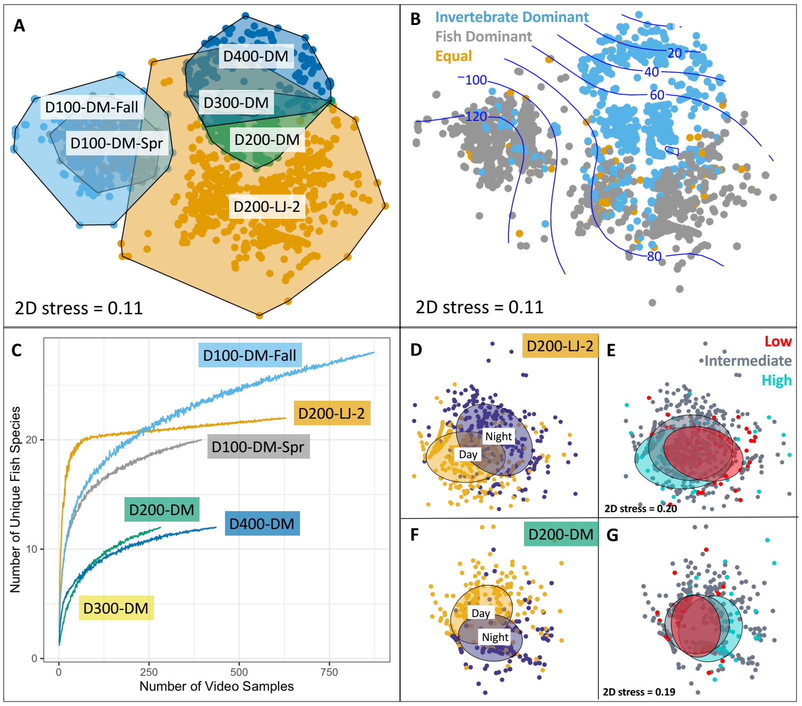

Figure 6: Seafloor community analyses using *DOV BEEBE* video samples. A) Non-metric multidimensional scaling (nMDS), plot showing seafloor community similarity across six deployments. Points represent Bray-Curtis similarity of square-root transformed counts of animals observed in each 20-second video sample (n = 3357) from each deployment (n = 6). Points are color-coded by deployment and a convex hull demarcates each deployment community. B) The same nMDS as in A) but points are color-coded by whether the seafloor community for each 20-second video sample was dominated by invertebrates (blue), vertebrates (gray), or an equal proportion of vertebrates and invertebrates (gold). Blue contours indicate relationship with oxygen concentration ($\mu mol\ kg^{-1}$). C) Species accumulation curves showing differences in fish diversity across deployments. D-G) Non-metric multidimensional scaling plots showing differences in seafloor community composition as a function of day versus night (D, F) and oxygen conditions (E, G) for two deployments: D200-LJ-2 (D, E) and D200-DM (F, G). In D) and F) yellow points represent daytime samples (6:00 AM – 5:59 PM) and purple points represent nighttime samples (6:00 PM – 5:59 AM). In E) and G), low (red) and high (blue) oxygen conditions represent the lowest and highest 10^{th} percentile of oxygen conditions encountered during each deployment time series. Ellipses represent grouping by category and show 50% confidence limits. 2D stress is the same for D) and E) and for F) and G). See Table 1 for camera deployment details.

Moved (insertion) [12]

Moved (insertion) [13]

We also looked at a community-level metric in relation to environmental oxygen conditions: community dominance by invertebrates or fishes. We hypothesized that higher-oxygen conditions would be characterized by fish dominance, compared to lower-oxygen conditions, which would be characterized by invertebrate dominance. Deployments D200-DM, D300-DM, and D400-DM were characterized by invertebrate dominance for either all or most (>98%) samples. In contrast, D200-LJ-2, D100-DM-Fall, and D100-DM-Spr were characterized by mixed communities, with fish-dominated communities more characteristic for D100-DM-Fall and D100-DM-Spr. In general, fish-dominated communities were more characteristic of higher-oxygen conditions when looking across all deployments (Fig. 6B), but we could not determine if this was specifically due to oxygen or other environmental covariates.

We were also able to examine differences in fish diversity across deployments using the Nanolander video samples. Species accumulations curves show differences in fish species diversity across deployments, with D100-DM-Fall having the highest number of observed fish species, followed by D200-LJ-2, D100-DM-Spr, and D200-DM and D400-DM which had the same number of unique fish species (Fig. 6C). The decline in fish diversity between D100-DM-Fall and D100-DM-Spr may be related to changes in environmental conditions between fall and spring, since the location is the same (Table 1).

Community-level changes within deployments were also examined for evidence of diurnal differences and differences related to oxygen concentration. D200-LJ-2 and D200-DM, which exhibited the highest oxygen variability and each had ~14-day time series of camera samples (Table 1, Fig. 6), were selected for further analysis. Clear diurnal differences were observed for both deployments (Fig. 6D, F), showing that at 200 m, communities are intimately linked to diurnal rhythms. Daytime communities were characterized by more combfishes (*Zaniolepis spp.*), hake (*M. productus*), small pelagic fishes such as the northern anchovy (*Engraulis mordax*), blacktip poachers (*X. latifrons*), and crabs (*Cancer spp.*), while nighttime communities were characterized by more lizardfish (*S. lucioceps*), spot prawns (*P. platyceros*), spotted ratfish (*H. colliei*), and hagfish (*E. stoutii*). Tuna crabs (*P. planipes*) and pink urchins (*S. fragilis*) showed no diurnal differences.

In contrast to clear diurnal differences, seafloor communities showed little evidence of responsiveness to changing oxygen conditions during the two deployments examined, however, some community-level differences do emerge when examining the highest and lowest oxygen conditions that were encountered during the deployment time series (Fig 6E, G). At ~200 m, crabs (*Cancer spp.*), spot prawns (*P. platyceros*), and lizardfish (*S. lucioceps*) were more common community members during the high oxygen extremes while tuna crabs (*P. planipes*) and Dover sole (*M. pacificus*) were more common during low oxygen extremes. For both deployments, the video time series lasted ~14 days, and a longer time series or more extreme oxygen variability may show more community-level differentiation in relation to oxygen extremes. Overall, our results show that at short-timescales (2 weeks or less), seafloor communities responded to diurnal differences more than to high-frequency oxygen variability.

4 Discussion

The California Current System is expected to experience the impacts of hypoxia and ocean acidification on seafloor communities sooner than many other regions of the world (Alin et al. 2012) because upwelling brings deep, oxygen-poor, and CO_2-rich waters into nearshore ecosystems along the US West Coast (Feely et al. 2008). Species in the SCB region may be

Deleted: rarefaction …iversity across deployments, with D100-DM-Fall having the highest number of observed fish species, followed by D200-LJ-2, D100-DM-Spr, D200-LJ-2,…nd D200-DM,…and D400-DM which had the same number of unique fish species (Fig. 4C…C). The decline in rarefaction ... [5]

Formatted: Font:12 pt

Moved up [12]: **plot showing seafloor community similarity across six deployments. Points represent Bray-Curtis similarity of square-root transformed counts of animals observed in each 20-second video sample (n = 3357) from each deployment (n = 6). Points are color-coded by deployment and a convex hull demarcates each deployment community. B) The same nM** ... [7]

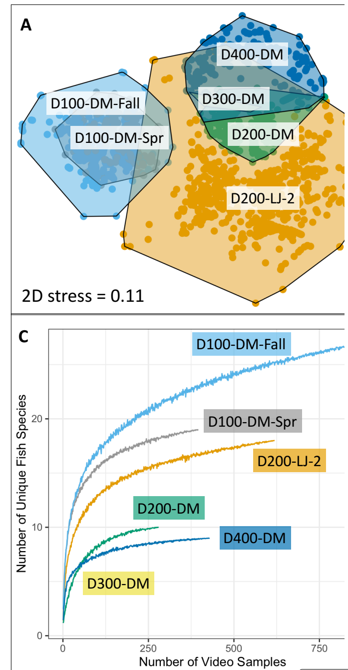

Deleted: ... [6]

Deleted: **rarefaction diversity across deployments.**

Moved up [13]: **D-G) Non-metric multidimensional scaling plots showing differences in seafloor community composition as a function of day versus night (D, F) and oxygen conditions (E, G) for two deployments: D200-LJ-2 (D, E) and D200-DM (F, G). In D) and F) yellow points represent daytime samples (6:00 AM – 5:59 PM) and purple points represent nighttime samples** ... [8]

Deleted: We were also able to examine community…ommunity-level changes within deployments to look at day/night…ere also examined for evidence of diurnal differences in seafloor communities …nd to examine if seafloor communities respond to high-frequency …ifferences related to oxygen variability…oncentration. D200-LJ-2 and D200-DM, which ... [9]

Deleted: 4E

particularly vulnerable to deoxygenation-induced habitat compression because the depth of the 22.5 µmol kg^{-1} oxygen boundary (i.e. upper OMZ boundary) occurs at a shallower depth than in northern California, Oregon, and Washington (Helly and Levin 2004, Moffitt et al. 2015). This study shows that even during the relaxed upwelling season, seafloor communities at ~400 m can be periodically exposed to OMZ conditions, communities at ~300 m are continuously exposed to hypoxic conditions, and communities at ~200 m are periodically exposed to hypoxic conditions. In the spring, upwelling of 13°C water (13CW) lowers oxygen conditions at 100 m, but conditions were never hypoxic in our study. Seafloor communities differed across the sampled environmental conditions, with communities living in lower-oxygen areas characterized by invertebrate dominance and decreased fish diversity.

4.1 Comparing oxygen variability: Short-term to long-term trends

Our Nanolander data show that at 100 m, benthic communities are exposed to ~4-7 µmol kg^{-1} differences in oxygen conditions at semidiurnal timescales and ranges of 7-34 µmol kg^{-1} at daily timescales (Supplement 1E, 1F). At ~200 m, benthic communities experienced higher oxygen variability of 10-12 µmol kg^{-1} at semidiurnal timescales and ranges of 15-46 µmol kg^{-1} at daily timescales (Supplement 1E, 1F). In contrast, semidiurnal and diurnal variability at 300 m and 400 m was reduced (Fig. 4, Table 1). At 300 and 400 m, a tidal signal still influenced oxygen conditions, but this signal was weaker and oxygen varied only ~2 µmol kg^{-1} at semidiurnal timescales (Supplement 1E). At daily timescales, oxygen varied between 8-15 µmol kg^{-1} at 300 m, and 3-12 µmol kg^{-1} at 400 m (Supplement 1F).

Across weekly timescales, at 100 m, oxygen conditions ranged by ~32 µmol kg^{-1} during deployment D100-DM-Spr and 46 µmol kg^{-1} during deployment D100-DM-Fall (Table 1). More extreme event-based decreases in oxygen have been reported near our study site at the Del Mar mooring (a continuous oceanographic monitoring mooring on the 100-m isobath; Nam et al. 2015), but were not captured during any of our deployments. At ~200 m, the range in oxygen conditions across weekly timescales was similar or higher than at 100 m and was 55 µmol kg^{-1} for D200-LJ-1, 59 µmol kg^{-1} for D200-LJ-2, and 40 µmol kg^{-1} for D200-DM. Similarly, the CV for oxygen was always higher during the 200 m deployments (13.72%, 12.92%, and 9.82%) compared to the 100 m deployments (5.07% and 5.72%) (Table 1). For the 300 m deployment, oxygen variability across weekly time-scales was lower than observed at ~200 m; the range in oxygen conditions was ~19 µmol kg^{-1} and the CV was 7.02% (Table 1). At 400 m, the range in oxygen conditions was ~17 µmol kg^{-1}, similar to 300 m, but the CV was higher (10.20%) because mean oxygen conditions were lower at this depth. High spatial resolution-sampling of the eastern tropical North Pacific OMZ documents considerable submesoscale oxygen variability with better oxygenated holes (Wishner et al. 2019); such patchiness could account for some of the variability we observed at ~400 m.

While we were only able to conduct one seasonal comparison, we observed that at 100 m, between the fall and spring deployments, mean oxygen conditions decreased from 132 to 104 µmol kg^{-1} (Table 1), and there was little overlap in the oxygen measurements across the two deployments (Fig. 4, Fig. 7E). The most extreme high-oxygen conditions observed during the spring deployment (D100-DM-Spr) were equivalent to the most extreme low-oxygen conditions observed during the fall deployment (D100-DM-Fall) (Fig. 4).

- **Deleted:** here
- **Deleted:** Input
- **Deleted:** Pacific Equatorial Water (PEW), which is brought up by the California Undercurrent, is key to determining near-seafloor
- **Deleted:** ~200 m, and in the spring, PEW upwells to
- **Deleted:** leading to lower oxygen
- **Deleted:** . In contrast, at deeper depths (~300 and 400 m), added input of PEW increases oxygen conditions.
- **Deleted:** differ
- **Formatted:** English (UK)
- **Deleted:** **short-term**
- **Deleted:** **of oxygen**
- **Deleted:** To compare the magnitude of natural O_2 variability over short time scales with reported trends of longer-term deoxygenation, we compared our results with the annual rates of oxygen loss reported for the SCB nearshore region (Bograd et al. 2008). From our
- **Deleted:** , we see
- **Deleted:** at daily time scales, semidiurnal and diurnal variability exposes
- **Deleted:** 1B). Across, weekly time-scales
- **Deleted:** experience a range of
- **Deleted:** conditions
- **Deleted:** ~32
- **Formatted:** Superscript
- **Deleted:** (D100-DM-Spr) –
- **Deleted:** (
- **Deleted:**). Between the fall and spring deployments, mean oxygen conditions decreased from 132 to 104 µmol kg^{-1} (Table 1). Even larger
- **Deleted:** at ~100 m (
- **Moved (insertion) [14]**
- **Deleted:**).
- **Deleted:** The rate of reported oxygen loss at ~100 m from 1984 to 2006 was

CalCOFI data from nearby station 93.3 28 provides additional context on the characteristics of oxygen variability across seasonal and interannual timescales. When temperature and oxygen profiles from ~16 years of quarterly CalCOFI cruises are examined, we see that the highest temperature variability occurs in the upper water column (<50 m) and variability below ~150 m is relatively low (Fig. 7A,B). In contrast, absolute oxygen variability (i.e. standard deviation) is greatest between 50-150 m (Fig. 7C), and the coefficient of variation for oxygen (CV) actually increases below 100 m (Fig. 7D).

Comparing our high-frequency Nanolander deployment results to oxygen measurements across these ~16 years of quarterly CalCOFI cruises, we observe that the range in oxygen measurements at ~100 m, 300 m, and 400 m only captured a small portion of the variability measured across the ~16 year time period. In contrast, for the ~200 m deployments, a significant fraction of the variance over seasonal and interannual time-periods was captured by the short-term deployments (Fig. 7E-H). Oxygen variability in the SCB is also affected by the El Niño Southern Oscillation (ENSO), with oxygen conditions lower during La Niña periods (Nam et al. 2011). During the Nanolander deployments (August 2017-March 2018), the monthly Niño-3.4 index was always negative (-0.21 to -1.04; cpc.ncep.noaa.gov) but weaker than the La Niña conditions described in Nam et al. (2011). Our deployments, therefore captured a neutral ENSO/weak La Niña state. Interannual variability due to ENSO is captured in the data distribution from the CalCOFI cruises.

Across multidecadal scales, dissolved oxygen at ~100 m in the SCB dropped from 1984 to 2006 at a rate of 1.25-1.5 μmol kg^{-1} year^{-1} (Bograd et al. 2008). Over a period of ~20 years, this rate of oxygen loss equates to the seasonal difference at 100 m between the spring upwelling season and the fall. Thus, if this rate of oxygen loss continues, in 20 years, fall conditions would resemble current spring conditions. At 200 m, oxygen declines of 1-1.25 μmol kg^{-1} year^{-1} loss have been reported (Bograd et al. 2008), suggesting that if this same rate of oxygen decline continues, the mean oxygen conditions at these depths (which ranged from ~70-82 μmol kg^{-1} from our data) will be continuously hypoxic in 10-20 years. Currently, communities are exposed to hypoxic conditions during the fall for <15% of the time in our time series (Table 1), but may experience hypoxic conditions more frequently in the spring. The greatest relative long-term changes in oxygen in the SCB have been reported at 300 m and represent an absolute change of 0.5-0.75 μmol kg^{-1} year^{-1} (Bograd et al. 2008). Conditions at 300 m were always hypoxic during our deployment, and may become more extreme in the future. At 400 m, oxygen decreases of 0.25-0.5 μmol kg^{-1} year^{-1} have been reported (Bograd et al. 2008), and if these trends continue, in 13-26 years, this depth zone may become the upper boundary of the OMZ.

Deleted: If

Deleted: , while spring conditions would be even lower (~75 μmol kg^{-1} mean [O_2]), potentially exposing communities at ~100 m to periodic hypoxic conditions, to which they are not currently exposed.
If mean conditions do become hypoxic at 200 m, the high variability we observed in environmental conditions at this depth may be advantageous to hypoxia intolerant members of the benthic community.

Moved (insertion) [15]

Moved (insertion) [16]

Deleted: If mean conditions do become hypoxic at 200 m, the high variability we observed in environmental conditions at this depth may be advantageous to hypoxia intolerant members of the benthic community.

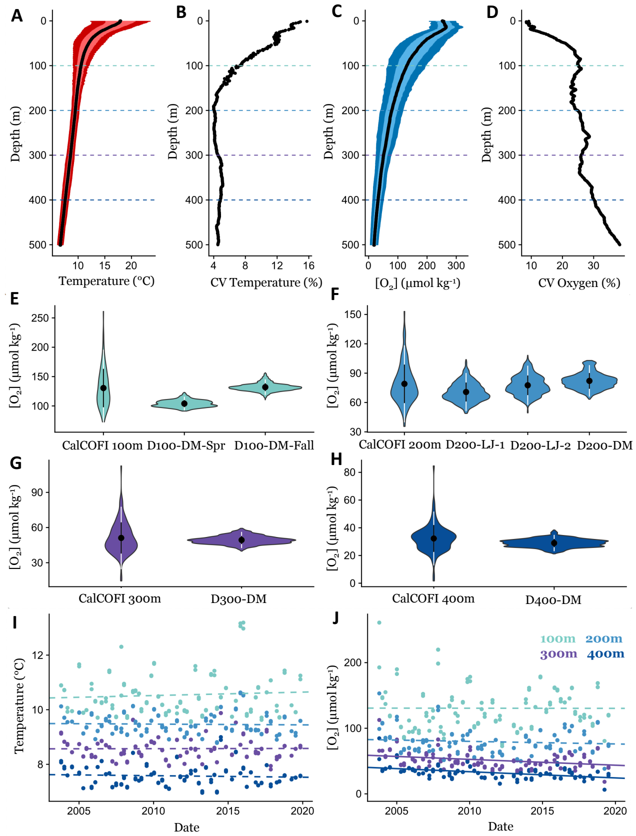

Figure 7: Comparing short-term environmental variability from *DOV BEEBE* deployments to longer-term trends using CTD casts at nearby CalCOFI station (93.3 28.0). Mean temperature (A) and oxygen (C) conditions through the water column (0-500 m) using CalCOFI CTD casts from Oct 2003-November 2019; light and dark colors indicate the variance around the mean and represent +/- 1 and 2 SD, respectively. Panels B and D show how the coefficient of variation (CV) for temperature and oxygen changes through the water column. Dotted lines in A-D indicate 100, 200, 300, and 400 m depths, and data are extracted for these depths for E-J. In E-H, violin plots show data distribution of oxygen measurements from ~16 years of CalCOFI quarterly cruises compared to ~3 week Nanolander deployments at 100 m (E), 200 m (F), 300 m (G), and 400 m (H). Violin plots show the mean +/- 1 SD (white) and +/- 2 SD (black). Panels I and J examine changes in temperature (I) and oxygen (J) conditions through time at 100, 200, 300, and 400 m. Dotted lines indicate non-significant linear relationships; solid lines indicate significant trends ($p < 0.05$).

Formatted: Caption, Indent: First line: 0"

Moved (insertion) [17]

Formatted: English (UK)

While we have related our results to reported trends for the SCB from Bograd et al. (2008), it is unclear if these trends will continue, since multidecadal oxygen trends associated with the Pacific Decadal Oscillation (PDO) may reverse (McClatchie et al. 2010). In the 1950s and 1960s, oxygen levels were also very low in the SCB, and conditions at ~250 m were as low or lower than those reported in the early 2000s (McClatchie et al. 2010). Additionally, projections for the California Current System suggest winds near the equatorward boundary may weaken as winds strengthen in the northern region (Rykaczewski et al. 2016) leading to less coastal upwelling and higher oxygen conditions in the SCB.

In recent years (2003-2019), at the CalCOFI station closest to the Nanolander deployments (93.3 28), no significant linear deoxygenation trends were detected at 100 or 200 m, but significant deoxygenation trends were detected for 300 and 400 m (300 m: LR, $R^2 = 0.10$, $p < 0.001$; 400 m: LR, $R^2 = 0.21$, $p < 0.001$) (Fig. 7J). No significant warming trends were detected at these depths during this period (Fig. 7I). At 300 m, oxygen declined by 0.89 µmol kg^{-1} $year^{-1}$ during the ~16 year time period, leading to a total oxygen loss of 14.25 µmol kg^{-1} across the time series, and at 400 m oxygen declined by 0.94 µmol kg^{-1} $year^{-1}$, leading to a total oxygen loss of 15.11 µmol kg^{-1} over the ~16 years. Comparatively, the range of oxygen conditions experienced over the ~3-week Nanolander deployment was ~19 µmol kg^{-1} at 300 m and ~17 µmol kg^{-1} at 400 m.

4.2 Implications of environmental variability for seafloor communities

A recent FAO report on climate change impacts to deep sea fish and fisheries (FAO 2018) developed an index of exposure to climate hazard, which represents the mean changes in an environmental variable relative to its historical variability (defined by the standard deviation in the historic period). Higher historic variability reduces the index of exposure to climate hazard. Other studies also suggest that conditions of higher environmental variability may have a protective effect on the vulnerability of species to climate change. Frieder et al. (2014) concluded that high-frequency pH variability was an underappreciated source of pH-stress alleviation for invertebrates that were sensitive to low pH conditions. In a hypoxic fjord, slender sole, *Lyopsetta exilis*, were also observed to persist for short periods under mean oxygen conditions that were lower than their critical oxygen threshold (P_{crit}), which was likely facilitated by high oxygen variability around the mean and movements in and out of critically hypoxic waters (Chu et al. 2018). Many marine fish species show physiological plasticity in metabolic rate, gill surface area, and blood-oxygen binding curves in relation to short-term changes in oxygen conditions (Mandic et al. 2009, Nilsson 2010, Richards 2010, Dubruzzi and Bennett 2014).

Based on our results, benthic communities at ~200 m may be partially buffered from the negative effects of deoxygenation due to the substantial high-frequency variability of oxygen experienced over daily and weekly timescales. While at 400 m overall oxygen variability is lower than at 200 m, the amount of oxygen variability relative to the mean is similar to that at 200 m, suggesting variability may provide some reprieve to benthic communities at 400 m from low mean oxygen conditions and deoxygenation trends. At 400 m, conditions were severely hypoxic ($O_2 < 22.5$ µmol kg^{-1}) for ~1% of the deployment time (Table 1), suggesting that even though this community is above the depth frequently associated with the upper boundary of the OMZ (450 m), it is already periodically exposed to OMZ conditions. Recent rapid deoxygenation trends at 400 m have also been observed at nearby CalCOFI station 93.3 28 from 2003-2019 (Fig. 7J).

Moved (insertion) [1]

Moved (insertion) [18]

Deleted: living

Deleted: apparently due to the presence of

Deleted: High-frequency variability of environmental

Deleted: could help buffer the negative effects of changing mean environmental conditions for benthic communities at 200 m.

Additionally, we note that between 200 and 300 m, there may be a boundary between two different water masses with implications for deoxygenation trends. The correlation between spiciness and oxygen concentration is negative at 200 m (indicative of high input of 13CW, which is a component of Pacific Equatorial Water, PEW), and then positive at 300 m (Fig. 5). Since changes in the volume of PEW have been implicated in the decreases in oxygen observed in the SCB (Booth et al. 2014, Bograd et al. 2015), it is worthwhile to note that increased input of this water mass could have a nonlinear effect on oxygen conditions in this area: increasing oxygen conditions at deeper depths, while decreasing them at shallower depths.

The high turbidity observed at 300 m may be due to shoaling and breaking nonlinear internal waves that can form bottom nepheloid layers (McPhee-Shaw 2006, Boegman and Stastna 2019). On the Peruvian margin, energy dissipation from tidally-driven internal waves have been shown to influence the distribution of epibenthic organisms by increasing suspension, transport, and deposition of food particles (Mosch et al. 2012). High turbidity conditions have also been observed during two separate ROV dives at ~340 m off Point Loma (unpublished, NDGallo), suggesting high turbidity conditions may be the norm at these depths on the upper slope in the SCB.

4.3 Observations of community responses to high-frequency environmental variability

Using *DOV BEEBE*, we were able to describe outer shelf and upper slope assemblages and examine if and how the seafloor community responds to O_2 variability at short timescales (daily, weekly, seasonal) in terms of community composition and diversity. Unexpectedly, we did not see strong evidence of seafloor community-level responses to daily and weekly oxygen variability. Seasonal differences were observed for D100-DM-Fall and D100-DM-Spr, but it is unclear if these were driven by oxygen, other upwelling-related environmental covariates such as temperature, pH, and productivity, or seasonal behavioral shifts associated with spawning or other activities.

Pronounced and rapid (< 2 week) community-level responses to hypoxia may occur in certain cases. For example, the Del Mar mooring has recorded strong event-based changes in dissolved oxygen (Nam et al. 2015) where oxygen rapidly increased or decreased over a short time-period (< 2 weeks). Rapid changes such as these that are outside of the typical regime of oxygen variability may lead to more immediate community responses. Unfortunately, we did not capture any such events during our deployments. Second, when oxygen conditions are near taxon-specific physiological thresholds, even small changes in oxygen can have large community-level effects (Levin et al. 2009, Wishner et al. 2018). In our deployments, spot prawn (*P. platyceros*) and crabs (*Cancer spp.*) were more strongly associated with the highest oxygen conditions during the D200-LJ-2 and D200-DM deployments, suggesting the oxygen conditions may be close to a critical threshold for these species. Tolerances to hypoxia are species-specific, with high intraspecies variability, so longer time series may better detect community-level changes. Given that we saw limited community-level responses at daily and weekly timescales, future deployments could sample less frequently (one camera sample taken every hour or every two hours) but over longer time periods (~4-8 weeks) to examine community-level responses to environmental variability.

Moved up [15]: The greatest relative long-term changes in oxygen in the SCB have been reported at 300 m and represent an absolute change of 0.5-0.75 µmol kg^{-1} $year^{-1}$ (Bograd et al.

Deleted: 2008). In contrast to the high environmental variability observed at 200 m, variability at 300 m was reduced and more similar to variability at 400 m (Fig. 2, Table 1). At daily timescales, a tidal signal still influenced oxygen conditions, which ranged ~2 µmol kg^{-1} (Supplement 1B). At weekly time scales, the range of oxygen conditions was ~19 µmol kg^{-1}, or ~39% of mean conditions at this depth (49.38 µmol kg^{-1}). Conditions at 300 m were always hypoxic, so these depths likely do not provide suitable habitat for hypoxia intolerant species under current conditions. ... [10]

Deleted: is an interesting depth which

Deleted: at an important

Deleted: 3

Deleted: The mechanism giving rise to the high turbidity observed at this depth also remains a mystery.

Formatted: Font:Times, Bold, Font color: Black, English (UK)

Deleted: **At 400 m, absolute variability of oxygen conditions was only slightly lower than that at 300 m (Table 1), but since the mean conditions were ~20 µmol kg^{-1} lower at 400 m, the relative variability in oxygen conditions was higher. At daily timescales, oxygen varied ~2 µmol kg^{-1} with the tides, and at weekly timescales, we observed a range of 17 µmol kg^{-1}, which represented 59% of the mean. Therefore, the amount of oxygen variability relative to the mean at 400 m, was similar to that at 200 m, suggesting that variability in oxygen conditions may provide some reprieve to benthic communities at this depth from low mean oxygen conditions. At this depth, we recorded severely hypoxic conditions (O_2 < 22.5 µmol kg^{-1}) for ~1% of the deployment time (Table 1), suggesting that even though this community is above the depth frequently associated with** ... [11]

Formatted: Caption, Indent: First line: 0"

Moved up [14]: **. High spatial resolution-sampling of the eastern tropical North Pacific OMZ documents consider** ... [12]

Deleted: **2019); such patchiness would not be unexpected off southern California. Oxygen decreases of 0.25-0.5 µmol** ... [13]

Moved up [16]: **2008), and if these trends continue, in 13-26 years, this depth zone may become the upper boundary** ... [14]

Moved up [17]: ... [15]

Formatted: English (UK)

Moved up [18]: Additionally, projections for the California Current System suggest winds near the equatorward bounda ... [17]

Deleted: In the 1950s and 1960s, oxygen levels were also very low in the SCB, and McClatchie et al. (2010) note that at ~2 ... [16]

Deleted: 2016).

Deleted: 2

Deleted: community-level responses may be observed if the mean environmental

Deleted: close to a critical threshold for a species that is dominant

Deleted: the community. Spot

The lack of community-level response to diurnal and weekly oxygen variability seen in our data may not be surprising given that animals have several ways that they can respond to stressful conditions, which would not affect community-level abundance, diversity, or composition patterns. For example, fish can become less active and reduce metabolic demands (Richards 2009, 2010), or can decrease feeding behavior (Wu 2002, Nilsson 2010) during periodic hypoxia. We observed that animals were less active in the deeper deployments, but it is unclear if this is due to the lower oxygen conditions or other environmental covariates.

5.0 Concluding remarks

Ocean deoxygenation is a global concern, with changes in oxygen conditions potentially impairing the productivity of continental shelves and margins that support important ecosystem services and fisheries. Nanolanders provide a powerful tool to examine short-term, fine-scale fluctuations in nearshore dissolved oxygen and other environmental parameters, and associated ecological responses that are rarely recorded otherwise. Oxygen variability was strongly linked to tidal processes, and contrary to expectation, high-frequency oxygen variability did not decline linearly with depth. Depths of 200 and 400 m showed especially high oxygen variability and seafloor communities at these depths may be more resilient to deoxygenation stress because animals are exposed to periods of reprieve during higher O_2 conditions and may undergo physiological acclimation during periods of low O_2 conditions at daily and weekly timescales. Despite experiencing high oxygen variability, seafloor communities showed limited responses to changing conditions at these short timescales. However, our deployments did not capture any large acute changes in environmental conditions that may elicit stronger community responses; future studies using this platform could allow for such observations.

The Nanolander *DOV BEEBE* is configured to collect paired physical, biogeochemical, and biological data in the deep-sea over multiple days, which is a rarity except for in areas with developed ocean observatories. We found that *DOV BEEBE* performed well over the course of the deployments, and allowed us to study seafloor community responses to short-term environmental forcing. Our deployment lengths were limited by battery capacity to power the LED lights; all other elements would have allowed for longer sampling duration. Specific ways to extend future deployment lengths are currently being explored and include: using higher efficacy LEDs, integrating additional batteries to power the LED lights into newly devised Nanolander side pods, improving circuit performance that powers the LED lights by using new camera controllers and solid-state relays, and using low-light cameras, such as the Sony 7S II, which reduce the light required to illuminate the field of view. Longer deployment lengths would be advantageous for capturing ecosystem responses to environmental variability across time-scales (hours to months).

Many of the areas where large decreases in oxygen have been observed occur in developing countries, such as along the western and eastern coast of Africa (Schmidtko et al. 2017). Large oxygen losses have also been observed in the Arctic (Schmidtko et al. 2017), where the seafloor habitat is understudied. Due to their compact design, small landers such as *DOV BEEBE* can provide a cost-effective and easily deployable tool for studying nearshore, deep-sea ecosystems and thus expand the capacity of developed and developing countries to monitor and study environmental changes along their coastlines. For

Deleted: **4.3 A global array of deep-sea landers**

Deleted:

Deleted: easy access to

Deleted: could

Deleted: capabilities

Deleted: We found that the Nanolander performed well and reliably over the course of the deployments, and was a valuable tool for studying environmental variability, describing seafloor communities, and linking seafloor community responses to environmental forcing. One advantage of the Nanolander design is that it is modular and easy to modify to fit the scope of research that is needed, and other sensors and instruments can easily be added.

continental margins and seafloor habitats, a global array of Nanolanders, similar in scope to the Argo program, could be envisioned. These would provide coupled physical, biogeochemical, and ecological measurements, which would greatly expand our understanding of temporal and spatial heterogeneity in nearshore deep-sea ecosystems and seafloor community sensitivity to environmental change.

Deleted: climate change impacts on
Deleted: communities

Code and data availability

Code and data are posted on Zenodo (10.5281/zenodo.3897966); publication will be timed with manuscript publication. It is intended that elements of the Nanolander design will be released as Open Source hardware in the future.

Deleted: will be made available through
Deleted: ; code and dataset
Deleted: acceptance and

Author contribution

NG, LL, KH, and NW designed the research plan; KH designed and built the Nanolander; NG, KH, and HY carried out the field deployments; NG, HY, and AN performed the video annotation and data analysis; NG wrote the manuscript and all authors contributed to editing the manuscript.

Deleted: design
Deleted: nanolander

Competing interests

Author Kevin Hardy is the owner of the company Global Ocean Design which currently sells Nanolanders similar to *DOV BEEBE*.

Deleted: nanolanders

Acknowledgements

This research was made possible through generous funding from several sources: the Mullin fellowship, Mildred E. Mathias Research Grant, the Edna B. Sussman Fellowship, the Mia J. Tegner Fellowship, Friends of the International Center Scholarship, the *DEEPSEA CHALLENGE* Expedition, the National Science Foundation Graduate Research Fellowship, and the Switzer Environmental Leadership Fellowship. Additionally, Global Ocean Design LLC provided internal R&D resources. The Fisheries Society for the British Isles and the UCSD Graduate Student Association provided travel support to present these results at scientific meetings. This work would not have been possible without the support of a tremendous number of people who helped with Nanolander deployments and recoveries, especially Phil Zerofski, Brett Pickering, Rich Walsh, Jack Butler, Mo Sedaret, Lilly McCormick, Andrew Mehring, Ana Sirovic, Rebecca Cohen, Ashleigh Palinkas, Jen McWhorter. I am forever grateful for the support of Javier Vivanco and others at Baja Aqua Farms for recovering and returning *DOV BEEBE* after it drifted into Mexican waters following an unsuccessful recovery. NG's Ph.D. committee members, B. Semmens, R. Norris, R. Burton, D. Victor, and R. Keeling, provided feedback on the research. We thank Kevin Stierhoff, SungHyun Nam, and one additional anonymous reviewer for feedback on the manuscript. NG is currently supported by a NOAA QUEST grant to B. Semmens.

References

Alin, S. R., Feely, R. A., Dickson, A. G., Hernandez-Ayon, J. M., Juranek, L. W., Ohman, M. D., and Goericke, R.: Robust empirical relationships for estimating the carbonate system in the southern California Current System and application to CalCOFI hydrographic cruise data (2005-2011), J. Geophys. Res., 117, C05033, 2012.

Bay, R. A., and Palumbi, S. R.: Multilocus adaptation associated with heat resistance in reef-building corals, Current Biology, 24, 2952-2956, 2014.

Beebe, W.: Half mile down, Harcourt, Brace and Company, New York, 344 pp, 1934.

Berg, P., Glud, R. N., Hume, A., Stahl, H., Oguri, K., Meyer, V., and Kitazato, H.: Eddy correlation measurements of oxygen uptake in deep ocean sediments, Limnol. Oceanogr.: Methods, 7, 576-584, 2009.

Boegman, L., and Stastna, M.: Sediment resuspension and transport by internal solitary waves, Annu. Rev. Fluid Mech., 51, 129-154, 2019.

Bograd, S. J., Castro, C. G., Lorenzo, E. D., Palacios, D. M., Bailey, H., Gilly, W., and Chavez, F. P.: Oxygen declines and the shoaling of the hypoxic boundary in the California Current, Geophys. Res. Lett., 35, L12607, 2008.

Bograd, S. J., Buil, M. P., Lorenzo, E. D., Castro, C. G., Schroeder, I. D., Goericke, R., Anderson, C. R., Benitez-Nelson, C., and Whitney, F. A.: Changes in source waters to the Southern California Bight, Deep-Sea Res. II, 112, 42-52, 2015.

Booth, J. A. T., Woodson, C. B., Sutula, M., Micheli, F., Weisberg, S. B., Bograd, S. J., Steele, A., Schoen, J., and Crowder, L. B.: Patterns and potential drivers of declining oxygen content along the southern California coast, Limnol. Oceanogr. 59(4), 1127-1138, 2014.

Chu, J. W. F., Curkan, C., and Tunnicliffe, V.: Drivers of temporal beta diversity of a benthic community in a seasonally hypoxic fjord, R. Soc. Open Sci, 5, 172284, 2018.

Dabruzzi, T. F., and Bennett, W. A.: Hypoxia effects on gill surface area and blood oxygen-carrying capacity of the Atlantic stingray, *Dasyatis sabina*. Fish Physiol. Biochem., 40(4), 1011-1020, 2014.

Doya, C., Aguzzi, J., Pardo, M., Matabos, M., Company, J. B., Costa, C., Mihaly, S., and Canals, M.: Diel behavioral rhythms in sablefish (*Anoplopoma fimbria*) and other benthic species, as recorded by the Deep-sea cabled observatories in Barkley canyon (NEPTUNE-Canada), Journal of Marine Systems, 130, 69-78, 2014.

Evans, Z. C., Boles, E., Kwiecinski, J. V., Mullen, S., Wolf, M., Devol, A. H., Moriyasu, R., Nam, S., Babbin, A. R., and Moffett, J. W.: The role of water masses in shaping the distribution of redox active compounds in the Eastern Tropical North Pacific oxygen deficient zone and influencing low oxygen concentrations in the eastern Pacific Ocean, Limnol. Oceanogr., 9999, 1-18, 2020.

Ewing, M., and Vine, A.: Deep-sea measurements without wires or cables, AGU Transactions, 19(1), 248-251, 1938.

FAO: Deep-ocean climate change impacts on habitat, fish and fisheries, Levin, L.A., Baker, M., and Thompson, A. (eds). FAO Fisheries and Aquaculture Technical Paper No. 638, Rome, FAO. 186 pp, 2018.

Feely, R. A., Sabine, C. L., Hernandez-Ayon, J. M., Ianson, D., and Hales, B.: Evidence for upwelling of corrosive "acidified" water onto the continental shelf, Science, 320, 1490-1492, 2008.

Flament, P.: A state variable for characterizing water masses and their diffusive stability: Spiciness, Prog. Oceanogr., 54, 493–501, 2002.

Frieder, C. A., Gonzalez, J. P., Bockmon, E. E., Navarro, M. O., and Levin, L. A.: Can variable pH and low oxygen moderate ocean acidification outcomes for mussel larvae?, Glob. Change Biol., 20(3), 754-764, 2014.

Frieder, C. A., Nam, S. H., Martz, T. R., and Levin, L. A.: High temporal and spatial variability of dissolved oxygen and pH in a nearshore California kelp forest, Biogeosciences 9, 3917-3930, 2012.

Gallo, N. D.: Influence of ocean deoxygenation on demersal fish communities: Lessons from upwelling margins and oxygen minimum zones, PhD. Dissertation, University of California, San Diego, 2018.

Gallo, N. D., Cameron, J., Hardy, K., Fryer, P., Bartlett, D. H., and Levin, L. A.: Submersible- and lander-observed community patterns in the Mariana and New Britain trenches: Influence of productivity and depth on epibenthic and scavenging communities, Deep-Sea Res. I, 99, 119-133, 2015.

Gallo, N. D., and Levin, L. A.: Fish ecology and evolution in the world's oxygen minimum zones and implications of ocean deoxygenation, Adv. Mar. Biol., 74, 117-198, 2016.

Gilly, W. F., Beman, J. M., Litvin, S. Y., and Robison, B. H.: Oceanographic and biological effects of shoaling of the oxygen minimum zone, Annu. Rev. Mar. Sci., 5, 393-420, 2013.

Helly, J. J., and Levin, L. A.: Global distribution of naturally occurring marine hypoxia on continental margins, Deep-Sea Res. I, 51, 1159-1168, 2004.

Henson, S. A., Beaulieu, C., Ilyina, T., John, J. G., Long, M., Séférian, R., Tjiputra, J., and Sarmiento, J. L.: Rapid emergence of climate change in environmental drivers of marine ecosystems, Nat. Commun., 8, 14682, 2017.

Hofmann, A. F., Peltzer, E. T., Walz, P. M., and Brewer, P. G.: Hypoxia by degrees: establishing definitions for a changing ocean, Deep-Sea Res. I, 58, 1212–26, 2011a.

Hofmann, G. E., Smith, J. E., Johnson, K. S., Send, U., Levin, L. A., Micheli, F., Paytan, A., Price, N. N., Peterson, B., Takeshita, Y., Matson, P., Crook, E. D., Kroeker, K. J., Gambi, M. C., Rivest, E. B., Frieder, C. A., Yu, P. C., and Martz, T. R.: High-frequency dynamics of ocean pH: a multi-ecosystem comparison, PLoS ONE 6(12), e28983, 2011b.

Jamieson, A.J.: Landers: Baited cameras and traps, In Biological Sampling in the Deep Sea, Ed. Malcolm R. Clark, Mireille Consalvey, and Ashley A. Rowden. John Wiley & Sons, Ltd, 2016.

Jamieson, A. J. Kilgallen, N. M., Rowden, A. A., Fujii, T., Horton, T., Lorz, A.-N., Kitazawa, K., and Priede, I. G.: Bait-attending fauna of the Kermadec Trench, SW Pacific Ocean: Evidence for an ecotone across the abyssal–hadal transition zone, Deep-Sea Res. I, 58, 49–62, 2011.

Juniper, S. K., Matabos, M., Mihaly, S., Ajayamohan, R. S., Gervais, F., and Bui, A. O. V.: A year in Barkley Canyon: A time-series observatory study of mid-slope benthos and habitat dynamics using the NEPTUNE Canada network, Deep-Sea Res. II, 92, 114-123, 2013.

Keller, A. A., Ciannelli, L., Wakefield, W. W., Simon, V., Barth, J. A., and Pierce, S. D.: Occurrence of demersal fishes in relation to near-bottom oxygen levels within the California Current large marine ecosystem, Fish. Oceanogr. 24(2), 162-176, 2015.

Kelley, D., and Richards, C.: oce: Analysis of Oceanographic Data, R package version 0.9-22, https://CRAN.R-project.org/package=oce, 2017.

Levin, L. A.: Manifestations, drivers, and emergence of open ocean deoxygenation, Ann. Rev. Mar. Sci., 10, 229-260, 2018.

Levin, L. A., Lieu, K.-K., Emeis, K.-C., Breitburg, D. L., Cloern, J., Deutsch, C., Giani, M., Goffart, A., Hofmann, E. E., Lachkar, Z.., Limburg, K., Liu, S.-M., Montes, E., Naqvi, W., Ragueneau, O., Rabouille, C., Sarkar, S. K., Swaney, D. P., Wassman, P., and Wishner, K. F.: Comparative biogeochemistry-ecosystem-human interactions on dynamic continental margins, Journal of Marine Systems, 141, 3-17, 2015.

Levin, L. A., Whitcraft, C. R., Mendoza, G. F., Gonzalez, J. P., and Cowie, G.: Oxygen and organic matter thresholds for benthic faunal activity on the Pakistan margin oxygen minimum zone (700 – 1100 m), Deep-Sea Res. II, 56, 449-471, 2009.

Long, M. C., Deutsch, C., and Ito, T. Finding forced trends in oceanic oxygen, Glob. Biogeochem. Cycles, 30, 381–397, 2016.

Lynn, R. J., and Simpson, J. J.: The California Current System: The seasonal variability of its physical characteristics, Journal of Geophysical Research, 92(C12), 12,947-12,966, 1987.

Mandic, M., Todgham, A. E., and Richards, J. G.: Mechanisms and evolution of hypoxia tolerance in fish, Proc. Biol. Sci., 276(1657), 735-744, 2009.

Matabos, M., Aguzzi, J., Robert, K., Costa, C., Menesatti, P., Company, J. B., and Juniper, S. K.: Multi-parametric study of behavioural modulation in demersal decapods at the VENUS cabled observatory in Saanich Inlet, British Columbia, Canada, Journal of Experimental Marine Biology and Ecology, 401, 89-96, 2011.

Matabos, M., Bui, A. O. V., Mihaly, S., Aguzzi, J., Juniper, S. K., and Ajayamohan, R. S.: High-frequency study of epibenthic megafaunal community dynamics in Barkley Canyon: A multi-disciplinary approach using the NEPTUNE Canada network, Journal of Marine Systems, 130, 56-68, 2014.

Matabos, M., Tunnicliffe, V., Juniper, S. K., and Dean, C.: A year in hypoxia: Epibenthic community responses to severe oxygen deficit at a subsea observatory in a coastal inlet, PLoS ONE 7(9), e45626, 2012.

McClatchie, S., Goericke, R., Cosgrove, R., Auad, G., and Vetter, R.: Oxygen in the Southern California Bight: Multidecadal trends and implications for demersal fisheries, Geophysical Research Letters, 37, L19602, 2010.

McPhee-Shaw, E.: Boundary-interior exchange: Reviewing the idea that internal-wave mixing enhances lateral dispersal near continental margins, Deep-Sea Res. II, 53(1-2), 42-59, 2006.

Meinvielle, M., and Johnson, G. C.: Decadal water-property trends in the California Undercurrent with implications for ocean acidification, J. Geophys. Res. Oceans, 118, 6687-6703, 2013.

Moffitt, S. E., Moffitt, R. A., Sauthoff, W., Davis, C. V., Hewett, K., and Hill, T. M.: Paleoceanographic insights on recent oxygen minimum zone expansion: lessons for modern oceanography, PLoS ONE, 10(1), e0115246, 2015.

Formatted: Font:MS Mincho

Mosch, T., Sommer, S., Dengler, M., Noffke, A., Bohlen, L., Pfannkuche, O., Liebetrau, V., and Wallmann, K.: Factors influencing the distribution of epibenthic megafauna across the Peruvian oxygen minimum zone, Deep-Sea Res. I, 68, 123–135, 2012.

Nam, S. H., and Send, U.: Direct evidence of deep water intrusions onto the continental shelf via surging internal tides, J. Geophys. Res., 116, C05004, 2011.

Nam, S., Takeshita, Y., Frieder, C. A., Martz, T., and Ballard, J.: Seasonal advection of Pacific Equatorial Water alters oxygen and pH in the Southern California Bight. J. Geophys. Res. Oceans 120, doi:10.1002/ 2015JC010859, 2015.

Nilsson, G. E.: Respiratory physiology of vertebrates: Life with and without oxygen, Cambridge University Press, New York, 334 pp, 2010.

Oksanen, J., Blanchet F. G., Friendly, M., Kindt, R., Legendre, P., McGlinn, D., Minchin, P. R., O'Hara, R. B., Simpson, G. L., Solymos, P., Stevens, M. H. H, Szoecs E., Wagner, H.: vegan: Community Ecology Package, R package version 2.4-4, https://CRAN.R-project.org/package=vegan, 2017.

Priede, I. G., and Bagley, P. M.: In situ studies on deep-sea demersal fishes using autonomous unmanned lander platforms, Oceanography and Marine Biology: an Annual Review, 38, 357-392, 2000.

Ren, A. S., Chai, F., Xue, H., Anderson, D. M., and Chavez, F. P.: A sixteen-year decline in dissolved oxygen in the Central California Current, Scientific Reports, 8, 7290, 2018.

Richards, J.: Metabolic and molecular responses of fish to hypoxia, Fish Physiol., 27, 443–485, 2009.

Richards, J.: Metabolic rate suppression as a mechanism for surviving environmental challenge in fish, Prog. Mol. Subcell. Biol., 49, 113–139, 2010.

Rykaczewski, R. R., Dunne, J. P., Sydeman, W. J., Garcia-Reyes, M., Black, B. A., and Bograd, S. J.: Poleward displacement of coastal upwelling-favorable winds through the 21st century, Geophys. Res. Lett., 42, 6424-6431, 2016.

Schmidtko, S., Stramma, L., and Visbeck, M.: Decline in global oceanic oxygen content during the past five decades, Nature, 542, 335-339, 2017.

Send, U., and Nam, S.: Relaxation from upwelling: the effect on dissolved oxygen on the continental shelf, J. Geophys. Res., 117, C04024, 2012.

Formatted: Font:MS Mincho

Tengberg, A., De Bovee, F., Hall, P., Berelson, W., Chadwick, D., Ciceri, G., Crassous, P., Devol, A., Emerson, S., Gage, J., Glud, R., Graziottini, F., Gundersen, J., Hammond, D., Helder, W., Hinga, K., Holby, O., Jahnke, R., Khiripounoff, A., Lieberman, S., Nuppenau, V., Pfannkuche, O., Reimers, C., Rowe, G., Sahami, A., Sayles, F., Schurter, M., Smallman, D., Wehrli, B., and De Wilde, P.: Benthic chamber and profiling landers in oceanography – A review of design, technical solutions and functioning, Prog. Oceanog., 35, 253-294, 1995.

Vaquer-Sunyer, R., and Duarte, C. M.: Thresholds of hypoxia for marine biodiversity, Proc. Natl. Acad. Sci. USA 105, 15452–57, 2008.

Wishner, K. F., Seibel, B., and Outram, D.: Ocean deoxygenation and copepods: Coping with oxygen minimum zone variability, Biogeosciences, https://doi.org/10.5194/bg-2019-394, 2019.

Wishner, K. F., Seibel, B.A., Roman, C., Deutsch, C., Outram, D., Shaw, C. T., Birk, M. A., Mislan, K. A. S., Adams, T. J., Moore, D., and Riley, S.: Ocean deoxygenation and zooplankton: Very small oxygen differences matter, Sci. Adv., 4, eaau5180, 2018.

Wu, R. S. S.: Hypoxia: from molecular responses to ecosystem responses, Mar. Pollut. Bull., 45, 35–45, 2002.